

2020

## Basigin as an Immune Mediator in the CNS

Alicia Gonzalez

University of North Florida, n01385305@unf.edu

Follow this and additional works at: <https://digitalcommons.unf.edu/etd>



Part of the [Immunity Commons](#), [Neuroscience and Neurobiology Commons](#), and the [Physiology Commons](#)

---

### Suggested Citation

Gonzalez, Alicia, "Basigin as an Immune Mediator in the CNS" (2020). *UNF Graduate Theses and Dissertations*. 975.

<https://digitalcommons.unf.edu/etd/975>

This Master's Thesis is brought to you for free and open access by the Student Scholarship at UNF Digital Commons. It has been accepted for inclusion in UNF Graduate Theses and Dissertations by an authorized administrator of UNF Digital Commons. For more information, please contact [Digital Projects](#).

© 2020 All Rights Reserved

BASIGIN AS AN IMMUNE MEDIATOR IN THE CNS

by

Alicia Gonzalez

A thesis submitted to the Department of Biology in partial fulfillment of the requirements

for the degree of Master of Science in Biology

UNIVERSITY OF NORTH FLORIDA

COLLEGE OF ARTS AND SCIENCES

## **Acknowledgements**

I would like to thank my advisor, Dr. Judith Ochrietor, for her guidance and support throughout my time at UNF. Without her, my experience in this program would not have been as pleasant. I would also like to thank my committee members, Dr. Beth Stotz-Potter and Dr. Fatima Rehman, for their suggestions that improved my work. Finally, I would like to thank my family for their continued support in my endeavors.

## Table of Contents

Figure Legend	iv – vi
Abstract	vii
Chapter 1: A Review of Basigin and Inflammation	1 – 9
Chapter 2: The Dynamics of Basigin in Response to LPS Through the Lifespan	10 – 34
Chapter 3: The influence of LPS on Basigin and TLR4 Transcription in the Retina	35 – 49
Chapter 4: Conclusion	50 – 51
References:	52 – 64
Vita:	65

## Figure Legend

Figure	Description	Page
Figure 1.1	<p><b>Signaling cascade of TLR4.</b></p> <p>TLR4 activates two pathways that mediate the production of inflammatory cytokines. The MyD88-dependent pathway requires the accessory protein TIRAP, while the TRIF-dependent pathway requires TRAM. MyD88 recruits IRAK proteins and TRAF6 for activation of the TAK1 complex by ubiquitination (Ub). TAK1 activates the IKK complex. The IKK complex phosphorylates I<math>\kappa</math>B proteins, initiating their degradation and allowing NF-<math>\kappa</math>B to dimerize and translocate into the nucleus. NF-<math>\kappa</math>B translocation activates transcription of inflammatory cytokines.<sup>59</sup></p>	3
Figure 1.2	<p><b>IL-6 mediated pathogenesis.</b></p> <p>(1) In the periphery, naïve T-cells are differentiated into Th17-cells after IL-6 stimulation. sIL-6R is released from the surface. (2) IL-6 stimulation of VCAM-1 increases the permeability of the blood brain barrier (BBB), allowing T-cells and IL-6 to cross into the central nervous system (CNS). (3) Differentiation of naïve T-cells and shedding of IL-6R in the central nervous system. (4) IL-17 secretion from Th17-cells resulting in a feedback loop with astrocytes as they produce IL-6 and reactive oxygen species (ROS). (5) Microglia and astrocyte activation by trans-signaling from IL-6 and sIL-6R. (6) ROS inducing demyelination of neurons.<sup>60</sup></p>	8
Figure 2.1	<p><b>Quantitative analyses of Basigin transcripts in neonate, adolescent, and adult mice.</b> Quantitative reverse transcription PCR was performed on RNA isolated from brain tissue incubated in DMEM <math>\pm</math> LPS for 3, 6, 12, or 24 hours of mice at PD 7 (A), PD 30 (B), and PD 180 (C) using primers complementary to Basigin. White bars represent tissue incubated with PBS as a control, while dashed bars represent tissue incubated in LPS. Error bars represent the coefficient of variation. * indicates a p-value <math>&lt; 0.05</math> by Tukey's HSD test, following a two-way ANOVA.</p>	18
Figure 2.2	<p><b>Quantitative analyses of Basigin protein in neonate, adolescent, and adult mice.</b> A direct ELISA for Basigin protein expression was performed using protein isolated from brain tissue incubated in DMEM <math>\pm</math> LPS for 3, 6, 12, or 24 hours of mice at PD 7 (A), PD 30 (B), and PD 180 (C). White bars represent tissue incubated with PBS as a control, while dashed bars represent tissue incubated in LPS. The runs were performed in duplicate. Error bars represent the standard error.</p>	19

Figure 2.3	<p><b>Quantitative analyses of TLR4 transcripts in neonate, adolescent, and adult mice.</b> Quantitative reverse transcription PCR was performed on RNA isolated from brain tissue incubated in DMEM ± LPS for 3, 6, 12, or 24 hours of mice at PD 7 (A) and PD 30 (B), using primers complementary to TLR4. White bars represent tissue incubated with PBS as a control, while dashed bars represent tissue incubated in LPS. Error bars represent the coefficient of variation. * indicates a p-value &lt; 0.05 by Tukey's HSD test, following a two-way ANOVA.</p>	21
Figure 2.4	<p><b>Localization and quantification of Basigin in PD 7 mouse brain tissue.</b> (A) Immunohistochemistry was performed on brain tissue sections of mice at PD 7 to localize the expression of Basigin (green). DAPI was used to stain nuclei (blue). (B) Quantification of the average fluorescence for each treatment is shown as a bar graph. White bars represent tissue incubated with PBS as a control, while dashed bars represent tissue incubated in LPS. Error bars represent standard error. * indicate a p-value &lt; 0.05 via a two-way ANOVA followed by a Tukey's HSD test.</p>	23
Figure 2.5	<p><b>Localization and quantification of Basigin in PD 30 mouse brain tissue.</b> (A) Immunohistochemistry was performed on brain tissue sections of mice at PD 30 to localize the expression of Basigin (green). DAPI was used to stain nuclei (blue). (B) Quantification of the average fluorescence for each treatment is shown as a bar graph. White bars represent tissue incubated with PBS as a control, while dashed bars represent tissue incubated in LPS. Error bars represent standard error. * indicate a p-value &lt; 0.05 via a two-way ANOVA followed by a Tukey's HSD test.</p>	24
Figure 2.6	<p><b>Localization and quantification of Basigin in PD 180 mouse brain tissue.</b> (A) Immunohistochemistry was performed on brain tissue sections of mice at PD 180 to localize the expression of Basigin (green). DAPI was used to stain nuclei (blue). (B) Quantification of the average fluorescence for each treatment is shown as a bar graph. White bars represent tissue incubated with PBS as a control, while dashed bars represent tissue incubated in LPS. Error bars represent standard error. * indicate a p-value &lt; 0.05 via two-way ANOVA followed by a Tukey's HSD test.</p>	25

Figure 2.7	<b>Localization of TLR4 in neonate, adolescent, and adult mouse brain tissue.</b>	27
	Immunohistochemistry was performed on brain tissue sections of mice at PD 7 (A), PD 30 (B), and PD 180 (C) to localize the expression of TLR4. The staining of TLR4 is shown in green (AF-488) was distributed sparingly within the tissue. DAPI (blue) was used to stain nuclei.	
Figure 2.8	<b>Localization of IL-6 in neonate, adolescent, and adult mouse brain tissue.</b>	29
	Immunohistochemistry was performed on brain tissue sections of mice at PD 7 (A), PD 30 (B), and PD 180 (C) to localize the expression of IL-6. The distribution of IL-6 (pseudo colored red, AF-488) was not found in abundance. DAPI (blue) was used to stain nuclei.	
Figure 3.1	<b>Quantitative analyses of Basigin-variant-1 transcripts in neonate, adolescent, and adult mice.</b>	42
	Quantitative PCR was performed on cDNA isolated from retinal tissue incubated in DMEM ± LPS for 3, 6, 12, or 24 hours of mice at PD 7 (A), PD 30 (B) and PD 180 (C), using primers complementary to B-v1. White bars represent tissue incubated with PBS as a control, while dashed bars represent tissue incubated in LPS. Error bars represent the coefficient of variation. * indicates a p-value < 0.05 by Tukey's HSD test, following a two-way ANOVA.	
Figure 3.2	<b>Quantitative analyses of Basigin-variant-2 transcripts in neonate, adolescent, and adult mice.</b>	44
	Quantitative PCR was performed on cDNA isolated from retinal tissue incubated in DMEM ± LPS for 3, 6, 12, or 24 hours of mice at PD 7 (A), PD 30 (B) and PD 180 (C), using primers complementary to B-v2. White bars represent tissue incubated with PBS as a control, while dashed bars represent tissue incubated in LPS. Error bars represent the coefficient of variation. * indicates a p-value < 0.05 by Tukey's HSD test, following a two-way ANOVA.	
Figure 3.3	<b>Quantitative analyses of TLR4 transcripts in neonate, adolescent, and adult mice.</b>	47
	Quantitative PCR was performed on cDNA isolated from retinal tissue incubated in DMEM ± LPS for 3, 6, 12, or 24 hours of mice at PD 7 (A), PD 30 (B) and PD 180 (C), using primers complementary to TLR4. White bars represent tissue incubated with PBS as a control, while dashed bars represent tissue incubated in LPS. Error bars represent the coefficient of variation. * indicates a p-value < 0.05 by Tukey's HSD test, following a two-way ANOVA.	

## Abstract

Chronic inflammation is a hallmark of many neurodegenerative disorders. Although the central nervous system (CNS) can stave peripheral pathogens from crossing the blood-brain barrier (BBB) through a network of continuous endothelia, astrocytes, and pericytes, prolonged exposure to a pathogen can compromise this barrier. Basigin, a cell adhesion molecule, is found on the surface of endothelial cells and has been demonstrated to interact with toll-like receptor 4 (TLR4). TLR4 recognizes lipopolysaccharide (LPS), found on the outer membrane of Gram-negative bacteria. The activation of TLR4 produces pro-inflammatory cytokines, like IL-6. The present study aims to address the expression pattern of Basigin gene products and TLR4 in brain and retinal tissue stimulated with LPS for a variation of time to mirror acute and chronic inflammation, as well as different life stages to determine whether the expression pattern is dynamic. Isolated brain tissue and neural retina from mice at postnatal day 7, 30 and 180 were incubated in DMEM  $\pm$  LPS for 3, 6, 12, or 24 hrs. Total RNA and protein were purified from the isolated tissue and used in quantitative reverse transcription PCR (qRT-PCR) and direct enzyme-linked immunosorbent assay (ELISA). Basigin, TLR4, and IL-6 were localized in brain tissue via immunohistochemistry. The results of the study suggest Basigin is highly expressed on microvasculature endothelial cells. The expression pattern of Basigin was not only dependent on length of exposure to LPS, but also age. Basigin's differential expression in 7- and 180-, but not 30-day old animals suggest pathogenic influence is more likely in neonatal and adult, but not adolescent mice. The pattern of TLR4 expression did not mirror that of Basigin gene products, indicating Basigin's role may not be to associate with TLR4, but may associate with other pro-inflammatory proteins, or may be acting in its role as an inducer of matrix metalloproteinases.

## Chapter 1 – A Review of Basigin and Inflammation

The immune system, a pathogenic defense mechanism, consists of two response pathways known as innate immunity and adaptive immunity. The innate immune system is the first line of defense and plays a critical role in activating and regulating the adaptive immune system.<sup>1,2</sup> The innate immune response is activated by biochemical signatures known as pathogen associated molecular patterns (PAMPs) within bacterial and fungal cell walls, which are detected by pattern-recognition receptors (PRRs) expressed on antigen presenting cells (APCs).<sup>3</sup> Four classes of PRRs have been characterized: Toll-like receptors (TLRs), C-type lectin receptors (CLRs), RIG-I-like receptors (RLRs), and nucleotide-binding oligomerization domain (NLRs) such as leucine-rich repeat-containing receptors. PAMP-mediated PRR induction leads to the activation of genes that express molecules such as cell adhesion molecules, immunoreceptors, cytokines and chemokines.<sup>4</sup>

As the first line of defense, the innate immune response is characterized as non-specific. The PRRs on granulocytes, dendritic cells, and macrophages (APCs) recognize and eliminate pathogens in a non-specific manner. However, if the innate response cannot eliminate the threat, the adaptive immune response is activated. Adaptive immunity acts in an antigen-specific response when presented with a pathogen.<sup>5</sup> The adaptive immune response utilizes small lymphocytes known as T cells and B cells. These lymphocytes originate in fetal bone marrow. T cells then migrate to the thymus for further development, followed by migration through the circulatory and lymphatic systems to secondary lymphoid tissues. These cells, now mature naïve T cells, wait until presented with specific antigens by APCs. B cells have a slightly different development in that these cells mature in the bone marrow. They also travel to secondary lymphoid tissues, but do not need formal antigen presentation to become active.

T lymphocytes and innate immune cells house TLRs along their plasma membrane. TLR4, specifically, recognizes lipopolysaccharide (LPS), of Gram-negative bacteria.<sup>6</sup> TLR4 consists of a single transmembrane alpha-helix and an extracellular domain that exhibits a leucine-rich horseshoe-like structure, characteristic of the leucine-rich repeat protein family (LRR).<sup>7</sup> The extracellular domain can be divided into three subdomains: N-terminal, central and C-terminal. The N-terminal and central domains play a role in charge pairing with lymphocyte antigen 96 (MD2), forming a heterodimer.<sup>8</sup> Cluster of Differentiation 14 (CD14) and LPS binding protein (LBP) are accessory proteins that enhance the detection of LPS by the TLR4-MD2 complex (Figure 1.1). As LPS forms aggregates in aqueous environments due to their amphipathic structure, LBP recognizes, binds and splits the aggregate into monomeric molecules prior to CD14 presentation.

The bound LPS is then transferred to the TLR4-MD2 heterodimer at the large hydrophobic binding pocket found within the  $\beta$ -cup fold structure of MD2.<sup>9-11</sup> Upon LPS transfer to the TLR4-MD2 complex, dimerization with a proximal TLR4-MD2 extracellular domain is achieved, triggering the recruitment of adaptor proteins to the intracellular domains and activating the transcription factors NF- $\kappa$ B and IRF3.<sup>12</sup> Each transcription factor is activated by the specific interaction of the adaptor proteins, MyD88, TIRAP, TRIF, and TRAM with each other and TLR4. The MyD88 pathway is mediated by TIRAP associating with TLR4, while the TRAM pathway is mediated by TRIF-TLR4 association (Fig. 1.1).<sup>13-16</sup> Though both pathways elicit transcription of cytokines, the focus will remain on the MyD88 pathway. Once MyD88 is activated, it interacts with several members of the IL-1 receptor-associated kinase (IRAK) family. IRAK4 is primarily activated, subsequently phosphorylating IRAK1.<sup>17,18</sup> Upon phosphorylation, IRAK4 and -1 dissociate from MyD88 and associate with TRAF6, an E3

ubiquitin ligase.<sup>19,20</sup> TRAF6 promotes polyubiquitination of itself, activating the I-kappa B kinase complex (IKK) which activates TAK1, resulting in the phosphorylation and degradation of inhibitory kappa B proteins (IκB), allowing NF-κB, a RelA–p50 heterodimer, to translocate into the nucleus and begin transcription of cytokines like IL-6.

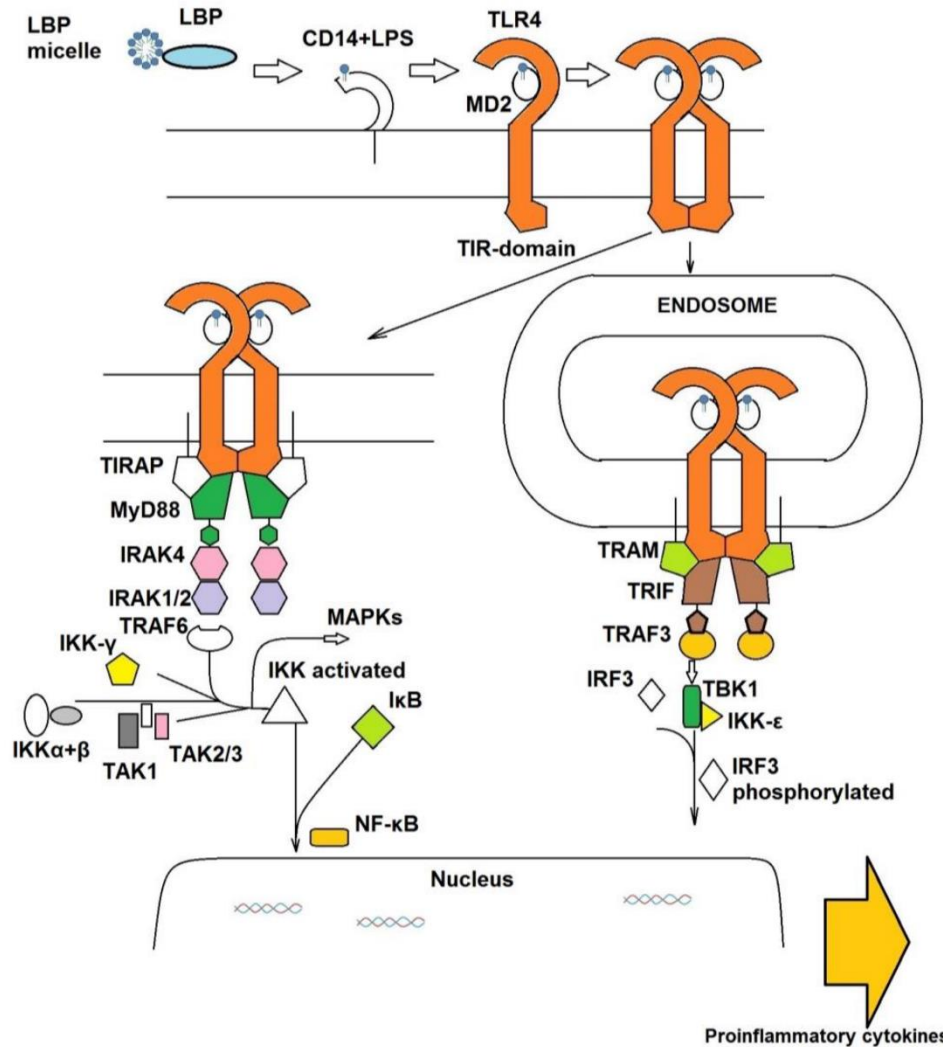


**Figure 1.1 Signaling cascade of TLR4.** TLR4 activates two pathways that mediate the production of inflammatory cytokines. The MyD88-dependent pathway requires the accessory protein TIRAP, while the TRIF-dependent pathway requires TRAM. MyD88 recruits IRAK proteins and TRAF6 for activation of the TAK1 complex by ubiquitination (Ub). TAK1 activates the IKK complex. The IKK complex phosphorylates IκB proteins, initiating their degradation and allowing NF-κB to dimerize and translocate into the nucleus. NF-κB translocation activates transcription of inflammatory cytokines.<sup>59</sup>

Cell adhesion molecules (CAMs) are proteins that line the surface of cells and play a role in cell-cell binding and communication. Four major superfamilies of CAMs have been identified and can be separated into two groups - calcium dependent and calcium independent CAMs. Cadherins, integrins, and selectins are those dependent on calcium, while the immunoglobulin superfamily is independent.<sup>21</sup> The immunoglobulin superfamily (IgSF) comprises cell surface and soluble proteins that contain a distinct immunoglobulin (Ig) domain. The domain possesses an immunoglobulin fold of 70-110 amino acids that form two opposing antiparallel  $\beta$ -sheets linked by a disulfide bridge which make up the core.<sup>22</sup> Beyond the core are constant (C-type) and variable (V-type) regions of immunoglobulins. The C-type domain can be further divided into C1- and C2-type domains.<sup>23</sup> Although C1-type domains can be found in immunoglobulins, T-cell receptors and major histocompatibility complex (MHC) proteins, C2-type domains are found in non-immunoglobulin-related molecules.

Basigin gene products are highly glycosylated transmembrane proteins and members of the IgSF. The Basigin gene contains eight exons which form two isoforms due to alternative splicing.<sup>24</sup> While both splice-variants contain an immunoglobulin-like extracellular domain, a single-pass transmembrane domain and short cytoplasmic tail, splice-variant-2 (B-v2) contains two immunoglobulin-like domains, encoded by exons 1-7.<sup>25</sup> Basigin-variant-1 (B-v1) contains three immunoglobulin-like domains and includes exon 1A (located between exon 1 and 2) within its coding region.<sup>24</sup> Although B-v2 is ubiquitously expressed, the B-v1 isoform is solely expressed on photoreceptor cells in the retina.<sup>24</sup> The role of B-v2 as a cell adhesion molecule is well characterized. However, studies have shown B-v2 also plays a role in behavior regulation, pro-inflammatory cytokine production, tumor metastasis, and regulation of cyclophilin signaling cascades.<sup>26</sup>

Both isoforms are capable of *cis*- and *trans*-recognition of molecules. Monocarboxylate transporters (MCTs), glucose transporter 1 (GLUT1), and cluster of differentiation 44 (CD44) are examples of proteins Basigin gene products associate with in *cis*. MCTs are expressed as 14 isoforms, though only MCT1-4 have been characterized to translocate energetically important monocarboxylates such as lactate, pyruvate, and ketone bodies.<sup>27</sup> Each isoform has been shown to have affinities for distinct substrates and inhibitors, in mammals.<sup>27</sup> The transmembrane domain and cytoplasmic tail of B-v2 tightly bind to and promote the expression of active MCT1, 3, and 4 within the plasma membrane.<sup>27,28</sup> The interaction between Basigin gene products and MCTs were demonstrated as essential for proper rod and cone function in the retina.<sup>29</sup> In the retina, lactate is used by photoreceptor cells for oxidative phosphorylation.<sup>30</sup> Excess lactate is transported out of the retina by MCT1 and MCT3 expressed on the retinal pigmented epithelium (RPE).<sup>31</sup> MCT1 is also highly expressed in Müller glial cells, photoreceptor cells, and vessels that form the blood-retina barrier.<sup>32</sup> Basigin gene products appear to be essential for proper metabolic processes necessary for retinal function. A lactate shuttle formed by the interaction of the B-v1/ MCT1 complex on the surface of photoreceptor cells and the B-v2/MCT1 complex expressed on the surface of Müller glial cells is thought to provide lactate to photoreceptor cells.<sup>33</sup> Without Basigin gene expression, MCT1 does not translocate to the plasma membrane and transport does not occur.<sup>28</sup>

Recent studies suggest that B-v2 plays a role in the innate immune system. A study conducted by the Fryer Laboratory at the Mayo Clinic Florida, showed that delivery of LPS to mice resulted in a two-fold increase in expression of Basigin-v2 in endothelial cells (John Fryer, personal communication). Further, a study conducted by Josephine Brown in the Ochriotor Laboratory at the University of North Florida determined the transmembrane domain of Basigin

gene products bind to TLR4 and is stabilized by both hydrophilic and hydrophobic interactions.<sup>34</sup> Although the transmembrane domain of Basigin gene products is mainly comprised of hydrophobic amino acids, a single glutamate residue also lies within the domain and is highly conserved among species.<sup>35</sup> It is thought that this residue interacts with the two histidine residues that lie within the transmembrane domain of TLR4.<sup>34</sup> It is possible that Basigin can stimulate the production of pro-inflammatory cytokines by its association with TLR4. Although the production of pro-inflammatory cytokines in an acute manner is not harmful, prolonged production, or chronic inflammation, can have deleterious effects on tissues - as in the case of chronic neuroinflammation.

Neuroinflammation can be brought on by many factors such as trauma, autoimmunity, or toxic metabolites. Within the central nervous system (CNS), microglia are the resident innate immune cells. The CNS is comprised of the brain, spinal cord, and the neural retina, which are protected by a specialized barrier, referred to here as the blood-CNS barrier (BCB). The BCB protects the CNS from circulating peripheral pathogens by a layer of endothelial cells contiguous by way of tight junction proteins.<sup>36</sup> Pericytes and astroglial end-feet form a second layer separating blood vessels from central nervous tissue and mediating the contact between tissue and circulating peripheral molecules.<sup>37</sup> These two layers are not in direct contact, rather there is some space separating them, known as the Virchow-Robin space.<sup>38,39</sup> Within the Virchow-Robin space, perivascular macrophages move about the interstitial fluid. The interaction and signaling that occurs between each cellular component is known as the neurovascular unit.

Endothelial cells are joined by tight junction proteins, which exhibit specific transport mechanisms and pinocytotic vesicles, thoroughly regulating the molecules that enter the central nervous system from the periphery. The transmembrane proteins that form cell-to-cell tight

junctions include claudins, occludin and junctional adhesion molecules (JAMs).<sup>40</sup> Cytoplasmic plaque proteins, such as cingulin and 7H6, provide a link between transmembrane proteins and the cytoskeleton of the cell. Additionally, they participate in intracellular signaling.<sup>41</sup> Though the tight junctions between endothelial cells inhibit the diffusion of polar solutes, the endothelial barrier is permeable to O<sub>2</sub>, CO<sub>2</sub>, N<sub>2</sub> and some gaseous anesthetics. Adsorptive and receptor-mediated transcytosis is used to regulate the entry of larger molecules that cannot freely cross the endothelial barrier.<sup>41</sup> Components of the innate immune system are also regulated by this barrier. Leukocyte recruitment and entry are mediated by a set of adhesion molecules expressed on the surface of leukocytes and endothelial cells, such as ICAM-1, VCAM-1 and PECAM-1.<sup>42,43</sup>

The integrity of the BCB can be disrupted through the upregulation of VCAM-1, induced by binding to very late antigen 4 (VLA-4) on activated T cells<sup>44,45</sup> or in response to peripheral IL-6.<sup>46</sup> IL-6 and transforming growth factor beta (TGF- $\beta$ ) have a dichotomous role in generating IL-17 producing T-helper 17 (Th17) cells from naïve T cells.<sup>47,48</sup> Disruption of the BCB allows for the infiltration of both naïve T cells and Th17 cells, and IL-6 into the CNS. As IL-6 concentration increases, T-cells become activated and shed their IL-6Rs through a metalloproteinase-mediated proteolytic cleavage, specifically by ADAM17.<sup>49</sup> The shedding of IL-6Rs leads to an increase in soluble IL-6Rs (sIL-6R).<sup>50</sup> This pool of soluble receptors provides an opportunity for trans-signaling and subsequent activation of microglia and astrocytes. Activation of microglia results in the release of reactive oxygen species (ROS), while activation of astrocytes results in an increased production of IL-6 as well as the production of ROS (Figure 1.2).<sup>51</sup> ROS ultimately leads to demyelination and degradation of neurons - the characteristic of neurodegenerative diseases such as Alzheimer's Disease, Parkinson's Disease, and Multiple Sclerosis.<sup>52-55</sup>

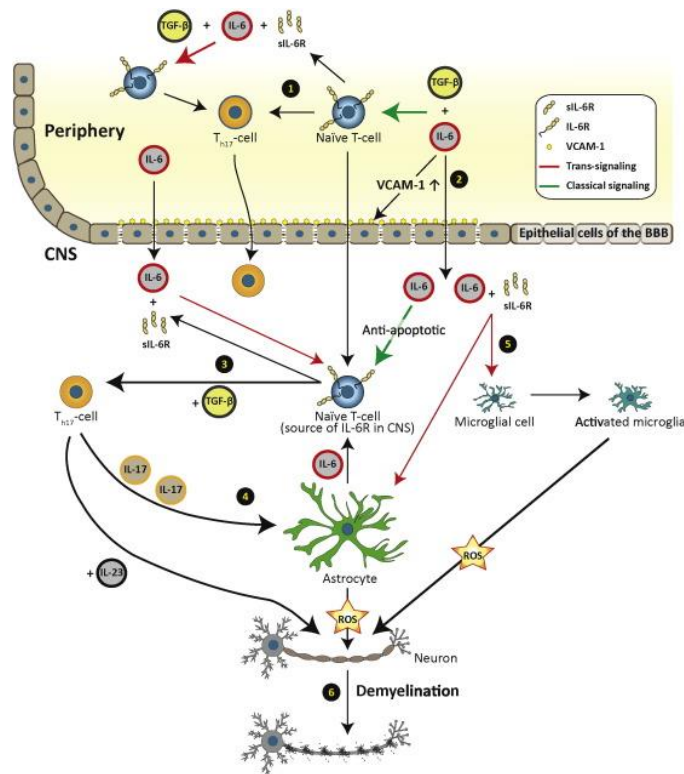


**Figure 1.2. IL-6 mediated pathogenesis.** (1) In the periphery, naïve T-cells are differentiated into Th17-cells after IL-6 stimulation. sIL-6R is released from the surface. (2) IL-6 stimulation of VCAM-1 increases the permeability of the blood brain barrier (BBB), allowing T-cells and IL-6 to cross into the central nervous system (CNS). (3) Differentiation of naïve T-cells and shedding of IL-6R in the central nervous system. (4) IL-17 secretion from Th17-cells resulting in a feedback loop with astrocytes as they produce IL-6 and reactive oxygen species (ROS). (5) Microglia and astrocyte activation by trans-signaling from IL-6 and sIL-6R. (6) ROS inducing demyelination of neurons.<sup>60</sup>

Essential polar molecules, such as glucose and amino acids, that cannot diffuse through the endothelial cell membrane are transported into the CNS via carrier-mediated transport. GLUT1, for example, is a crucial insulin independent glucose transporter that is expressed on endothelial cells, astrocytes and the choroid plexus.<sup>56</sup> Regulation of GLUT1 expression is necessary to maintain proper glucose concentration within neural tissue. Polar amino acids are also necessary to synthesize neurotransmitters such as serotonin and dopamine. The concentration and synthesis of these molecules have been correlated to the rate at which they cross the endothelial barrier.<sup>57</sup> Solute carriers (SLCs), expressed on the cell membrane of

endothelial cells, provide the transport mechanism to preserve the delicate balance of glucose and amino acids neural tissue needs to sustain its function.<sup>58</sup>

The introduction of a peripheral pathogen can pose a detriment to the CNS by disruption of the BCB or to crucial metabolic mechanisms that sustain the central environment. This study aims to investigate the role of Basigin gene products and its potential association to TLR4 in response to an inflammatory stimulus, lipopolysaccharide (LPS). Upon varying lengths of exposure to LPS, the expression pattern of Basigin gene products, TLR4, and IL-6 was determined in the brain and neural retina, ex-vivo. Additionally, this study aims to determine whether these expression patterns change throughout the lifespan using a murine model, as the proteins of interest are highly similar to those in humans. Investigating the role Basigin plays in neuroimmunity will expound the complexity of neurodegenerative disorders.

## Chapter 2 – The Dynamics of Basigin in Response to LPS Through the Lifespan

About one third of Americans suffer from one of the more than 600 neurological disorders at some point in their life, according to the National Institute of Neurological Disorders and Stroke. As the life expectancy of the United States population increases<sup>61</sup>, so do the number of cases of late-onset neurological disorders, like neurodegenerative diseases.<sup>62-64</sup>

Neurodegenerative diseases are categorized as the progressive loss of neuronal structure and function, resulting in neuronal cell death. The majority of neurons, the primary cells of the central nervous system (CNS), are nonmitotic, thus damage to these cells are detrimental to the organ system and require protection from peripheral pathogens. Additionally, maintenance of the central metabolic and ionic environment is highly important to ensure proper function.

Chronic inflammation is a hallmark of many neurodegenerative diseases. Glial cells, thought of as the supporting cells of the CNS, provide a means of clearance for infections or toxins.<sup>65</sup> The introduction of these harmful stimuli activates the resident macrophages of the CNS, microglial cells. Activated microglia have a phagocytotic phenotype and release inflammatory mediators like chemokines and cytokines.<sup>65</sup> Though the acute onset of these innate immune cells does not lead to long-term detriments, their sustained activation does.<sup>66,67</sup>

Microglia produce reactive oxygen species (ROS) through peroxidases inside the cell, oxidative processes of mitochondria, or most commonly, NADPH oxidase on the membrane surface.<sup>68,69</sup> Interestingly, NADPH oxidase is not presented on the cell surface until the phagocyte has been exposed to specific stimuli, such as bacteria and inflammatory peptides.<sup>70</sup> Once on the cell surface, the active enzyme complex transports electrons from NADPH within the cytoplasm to extracellular oxygen, generating superoxide ( $O_2^-$ ).<sup>71</sup> The increasing concentration of  $O_2^-$  allows for membrane lipid peroxidation to occur.<sup>72</sup> The damaged neuron

then releases neuroglial activators, such as  $\mu$ -calpain, matrix metalloproteinase 3,  $\alpha$ -synuclein, and neuromelanin, perpetuating the cycle of neuronal degradation.<sup>73-75</sup> This cycle of microglia activation and subsequent neuronal attack is referred to as microgliosis.

Though microgliosis can be maintained by sustained inflammatory responses within the CNS, immune mediators from the periphery can also contribute to neuronal damage. Under normal homeostatic conditions, the blood-CNS barrier (BCB) mediates the movement of molecules and ions from the periphery into the CNS. However, peripheral cytokines, like interleukin-6 (IL-6) can upregulate the expression of vascular cell adhesion molecule-1 (VCAM-1), found on the surface of leukocytes and endothelial cells<sup>40,41,44</sup>, resulting in the disruption of the BBB. Infiltration of IL-6 subsequently activates microglia.<sup>76</sup>

A number of cell adhesion molecules are expressed on the surface of endothelia forming the BBB, including Basigin.<sup>77,78</sup> The immunoglobulin glycoprotein has been demonstrated to have both neuroprotective and neurodegenerative function.<sup>26</sup> Basigin acts as a signaling receptor for cyclophilin A (CypA), mediating the recruitment of leukocytes to injured or infected tissues.<sup>79</sup> However, a rapid influx of leukocytes, due to the chemotactic potency of CypA, can contribute to inflammation.<sup>80</sup> Moreover, Basigin associates with a variety of proteins involved in inflammation like E-selectin, Toll-like Receptor 4 (TLR4) and Cluster of Differentiation 44 (CD44), a lymphocyte homing receptor.<sup>34,81-83</sup>

TLR4 is a member of the toll-like receptor class of proteins that recognize invading organisms possessing pathogen associated molecular patterns (PAMPs). TLR4 has been demonstrated to specifically recognize lipopolysaccharide (LPS) of Gram-negative bacteria<sup>6</sup>, and is expressed on T lymphocytes, macrophages, and endothelial cells.<sup>84-86</sup> Upon LPS recognition,

TLR4 dimerization occurs, followed by a phosphorylation cascade that results in the transcription of pro-inflammatory cytokines, such as IL-6.

A previous study conducted by this laboratory has shown an association between Basigin and TLR4, *in vitro*.<sup>34</sup> To further elucidate Basigin's role in neuroinflammation, this study aims to quantify and localize the expression of Basigin and TLR4 within neonate, adolescent, and adult brain tissue after acute and chronic inflammation. It is hypothesized the Basigin gene expression increases in response to LPS, as seen by the Fryer Laboratory at the Mayo Clinic Florida (John, Fryer, personal communication).

## **Materials and Methods**

### **Animals**

All experiments described in the present study were approved by the University of North Florida Institutional Animal Care and Use Committee (IACUC) under protocols #17-003 and #19-008 and were conducted in accordance with the American Veterinary Medicine Association (AVMA). Mice were housed at the University of North Florida vivarium in accordance with institutional requirements for animal care and were maintained under a standard 12:12 h light/dark cycle and were allowed *ad libitum* access to 8604 Harlan Teklad Rodent Chow (Harlan Research Models and Services, Indianapolis, IN) and water.

### **Treatment of Tissue**

Brain tissue was dissected from female and male wild-type C57/129 hybrid mice<sup>87</sup> at postnatal days (PD) 7, 30, and 180. Three brains were collected for each age group. Dissected brains from PD 7 mice were sectioned along their midsagittal plane, while PD 30 and 180 brains were sectioned into four equal sagittal parts. Each section was incubated in DMEM + PBS or LPS (10 µg/mL; InvivoGen, San Diego, CA) at 37°C with 5% CO<sub>2</sub> for 3, 6, 12, or 24 hours.

Incubation periods for each treatment were performed in triplicate for all age groups. Following incubation, half of each brain sample was preserved by immersion-fixation in 4% paraformaldehyde in phosphate-buffered saline for 24 hours at 4°C, followed by incubation in 100% ethanol at -20°C, while the other half was directly frozen at -80°C.

### **RNA and Protein Isolation**

Frozen brain tissue was homogenized in extraction solution (TRI Reagent; Molecular Research Center, Cincinnati, OH). A 500 µL sample was used to isolate total RNA, following the instructions of the manufacturer and solubilized in Milli-Q water. The concentration of RNA was determined spectrophotometrically at 206 nm (Biotek Instruments, Winooski, VT).

Proteins were then isolated from the organic phase and solubilized in 1% SDS, following the instructions of the manufacturer. A Bradford Coomassie protein assay (Pierce Biotechnology, Rockford, IL, USA) was used to determine the concentration of isolated protein. A standard curve was generated using serial dilutions of bovine serum albumin (BSA) from 0.2 mg/mL to 2.0 mg/mL. Spectrophotometric analysis was performed at 595 nm (Biotek Instruments, Winooski, VT).

### **Quantification of Basigin and TLR4 mRNA Expression**

The isolated total RNA was used to quantify the expression of Basigin and TLR4 in PD 7 and 30 mouse brain tissue. Amplification of reverse-transcribed cDNA was detected in one-step using a nucleic acid fluorogenic dye (SYBR Green; iUniversal, Bio-Rad, Inc.) and primers complementary in sequence to the cDNA of Basigin, TLR4 and mouse 18S ribosomal RNA. The RNA isolated from PD180 mice was reverse transcribed to cDNA (iScript™ cDNA Synthesis Kit, Bio-Rad, Inc.), which was then used to perform quantitative PCR (SsoAdvanced Universal SYBR Green Supermix, Bio-Rad, Inc.), including the aforementioned primer sets. The primer

sequences used are as follows: Basigin Fwd 5' – CTGCGCGGCGGGCACCAT; Basigin Rvs 5' – GCTGTTCAAAGAGCAGGTAAGCT; TLR4 Fwd 5' – CACCGTGATTGTG-GTATCCACTGT; TLR4 Rvs 5' – GTCCTCATTCTGACTCGAGTAGAT; 18S Fwd 5' – AGT-CCCTGCCCTTTGTACACA; 18S Rvs 5' – CCGAGGGCCTCACTAAACC. Although Basigin and 18S sequences were already established<sup>24</sup>, the primer sequence complimentary to TLR4 was designed using NCBI's Primer-BLAST software in conjunction with the GenBank TLR4 sequence (accession: NM\_021297.3). All runs were performed in triplicate using a CFX Connect Real-Time PCR Detection System (Bio-Rad, Inc.) and included standard melt curve analyses. Thermal cycling protocols were set according to the manufacturer. The amount of each amplified product was calculated using a standard curve generated for each primer set. Expression of Basigin and TLR4 were normalized to 18S ribosomal RNA expression. Prior to analysis via a two-way ANOVA, the quantified mRNA was transformed by taking the square-root to ensure normality.

### **Protein Expression of Basigin**

Protein expression of Basigin was determined by performing a direct enzyme-linked immunosorbent assay (ELISA), using the total protein isolated from mouse brains. Wells of a clear, flat-bottom 96-well plate were coated with serial dilutions of recombinant Basigin (Mouse Basigin Protein Recombinant, LifeSpan BioSciences, Inc., Seattle, WA) from 500 ng/mL to 7.8125 ng/mL or 10 µg of isolated mouse brain protein, in duplicate. The plate was incubated overnight at 4°C. All protein was then removed, and each well was washed 3 times with approximately 200 µL of PBS containing 0.05% Tween-20 (PBS-T). The wells were then incubated at 37°C for 30 minutes with 100 µL of a BSA solution, diluted 1:10 in PBS. The BSA solution was removed and the wells were washed 3 times with PBS-T. A 100 µL volume of

affinity-purified rabbit anti-Basigin<sup>24</sup> (diluted 1:500 in PBS) was added to the wells and incubated at 37°C for 30 minutes. The primary antibody was removed, and the wells were washed 3 times with PBS-T. The wells were then incubated with 100 µL of alkaline phosphatase-conjugated goat-anti-rabbit secondary antibody (AP-GAR; Pierce/ThermoScientific; diluted 1:1000 in PBS) at 37°C for 30 minutes, followed by a removal of the unbound secondary antibody from the wells and washing of the wells with PBS-T 3 times. One hundred microliters of AP substrate (PNPP; Thermo Fisher Scientific, Rockford, IL) was added to each well and incubated at room temperature for 30 minutes. The reaction was stopped by the addition of 2N NaOH and the absorbance at 405 nm was measured on a Bio-Tek plate reader (Biotek Instruments). The duplicate measurements were averaged. The average recombinant Basigin measurements were then used to create a standard curve, which was used to determine the concentration of Basigin within brain tissue samples. A two-way ANOVA was used to determine the influence of incubation period and age on the expression of Basigin.

### **Immunohistochemistry**

Paraformaldehyde-fixed tissues were processed into paraffin-embedded blocks, followed by preparation of 5 µm thick sagittal sections using a rotary microtome, adhered to microscope slides coated with 0.01% poly-l-lysine (Sigma Aldrich, St. Louis, MO).

Indirect immunofluorescence detection was performed to localize Basigin, TLR4, and IL-6. Prior to incubation with the protein-specific antibody, the sections were incubated in a limonene-based xylene substitute (CitriSolv™, Fisher Scientific, Fair Lawn, NJ) 2 times for 10 minutes to remove the paraffin wax. The sections were rehydrated by incubation in each concentration of ethanol for 5 minutes, 100%, 95%, and 70%, followed by tris-buffered saline (TBS). Each section was encircled using a hydrophobic barrier pen (Super PAP Pens: Liquid

Blocker, Ted Pella, Inc.). The tissue sections were then incubated in a blocking solution of TBS containing 2% normal goat serum and 1.5% Triton X-100 in a humidified chamber overnight at 4°C. An antibody solution containing either rabbit anti-Basigin<sup>24</sup>, rabbit anti-TLR4 (Thermo Fisher Scientific, Rockford, IL), or rabbit anti-IL-6 (Thermo Fisher Scientific, Rockford, IL), diluted 1:100 in the blocking solution was incubated with the tissue for 30 minutes in a humidified chamber at 37°C, followed by an overnight incubation at 4°C. The tissue sections were washed 10 times in TBS and incubated in a FITC-conjugated goat anti-rabbit secondary antibody (Thermo Fisher Scientific, Rockford, IL) diluted 1:250 in blocking solution for 30 minutes in a humidified chamber at 37°C. The tissues were incubated with DAPI (Thermo Fisher Scientific, Rockford, IL) diluted 1:1000 in TBS for 5 minutes at room temperature and then washed with several changes of TBS. Coverslips were mounted with TBS/glycerol (1:1) containing p-phenylenediamine (Sigma-Aldrich, St. Louis, MO). An Olympus FV1000 microscope was used to visualize the tissue. Software associated with the instrument was used to perform densitometry analyses by quantifying the fluorescence of each protein tested. A two-way ANOVA was used to determine the influence of incubation period and age on the expression of those proteins.

## **Results**

### **Expression of Basigin**

To determine whether Basigin expression varies in brain tissue of neonatal, adolescent, and adult mice when subjected to an acute and chronic inflammatory stimulus, transcripts and proteins were analyzed. Basigin transcripts in mouse brain tissue collected at PDs 7, 30, and 180 and incubated for several time points indicated that in all age groups, Basigin transcripts were most abundant at the 3-hour time point, then decreased as incubation time increased, regardless

of treatment (Figure 2.1). Statistical analyses indicated that incubation time, but not treatment, affected Basigin transcript expression for mice at PDs 7 and 30. A similar trend was observed for mice at PD 180. No statistical significance between PBS and LPS treated groups at both PD 7 and 30 ( $p = 0.976$ ;  $0.978$ ) was observed. However, Basigin transcription of PD 7 tissues incubated for 3 hours was significantly higher ( $p = 2.59 \times 10^{-5}$ ) than that of transcript levels for tissues of the same age incubated at other time points. Similarly, mice at PD 30 showed significant differences in Basigin transcript levels for incubation periods ( $p = 0.002$ ), in which tissues incubated for 3 hours expressed Basigin significantly more than that of tissues incubated for 12 and 24 hours, while tissues incubated for 6 hours expressed significantly more Basigin than tissues incubated for 24 hours. No statistical significance was determined for the P180 data.

Protein expression of Basigin in mouse brain tissue at different ages, post treatment was quantified by ELISA. A trend was observed in which Basigin protein was elevated in brain tissue of PD 7 and 30 mice incubated in PBS for 24 hours. This was not observed in PD 180 mice. No significant difference in Basigin expression was observed between tissues treated with PBS or LPS ( $p = 0.168$ ) for mice at PD 7 (Figure 2.2A;  $n = 3$ ). Further, incubation periods did not produce significant differences in Basigin expression ( $p = 0.145$ ), nor was there a significant interaction effect for this age group ( $p = 0.123$ ). Similar results were observed for mice at PD 30, and PD 180 (Figure 2.2B and C, respectively;  $n = 3$ ), where neither treatment ( $p = 0.43$ ;  $0.947$ ) nor incubation period ( $p = 0.205$ ;  $0.996$ ) showed significant differences in Basigin expression. An interaction effect was not observed for either age group ( $p = 0.078$ ;  $0.844$ ).

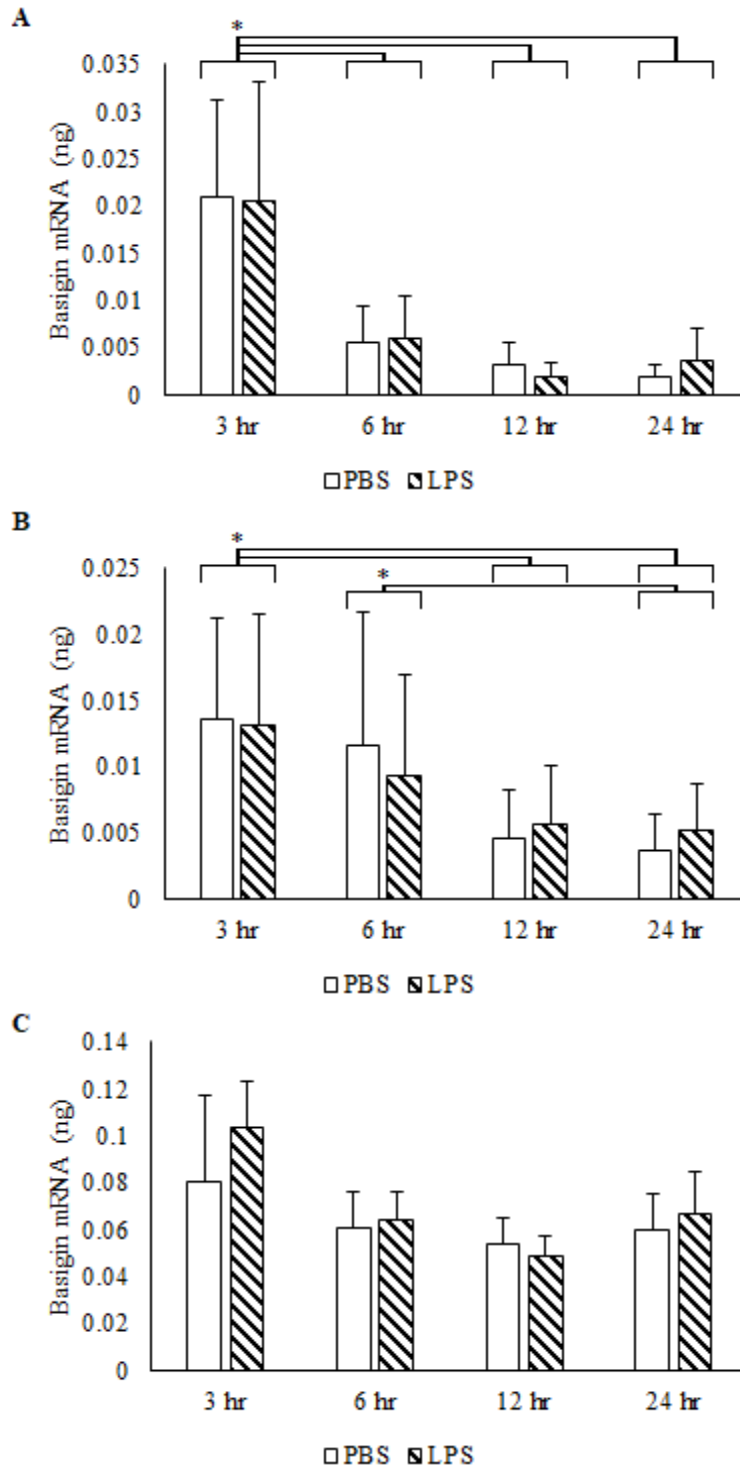


**Figure 2.1 Quantitative analyses of Basigin transcripts in neonate, adolescent, and adult mice.** Quantitative reverse transcription PCR was performed on RNA isolated from brain tissue incubated in DMEM  $\pm$  LPS for 3, 6, 12, or 24 hours of mice at PD 7 (A), PD 30 (B), and PD 180 (C) using primers complementary to Basigin. White bars represent tissue incubated with PBS as a control, while dashed bars represent tissue incubated in LPS. Error bars represent the coefficient of variation. \* indicates a p-value  $<$  0.05 by Tukey's HSD test, following a two-way ANOVA.

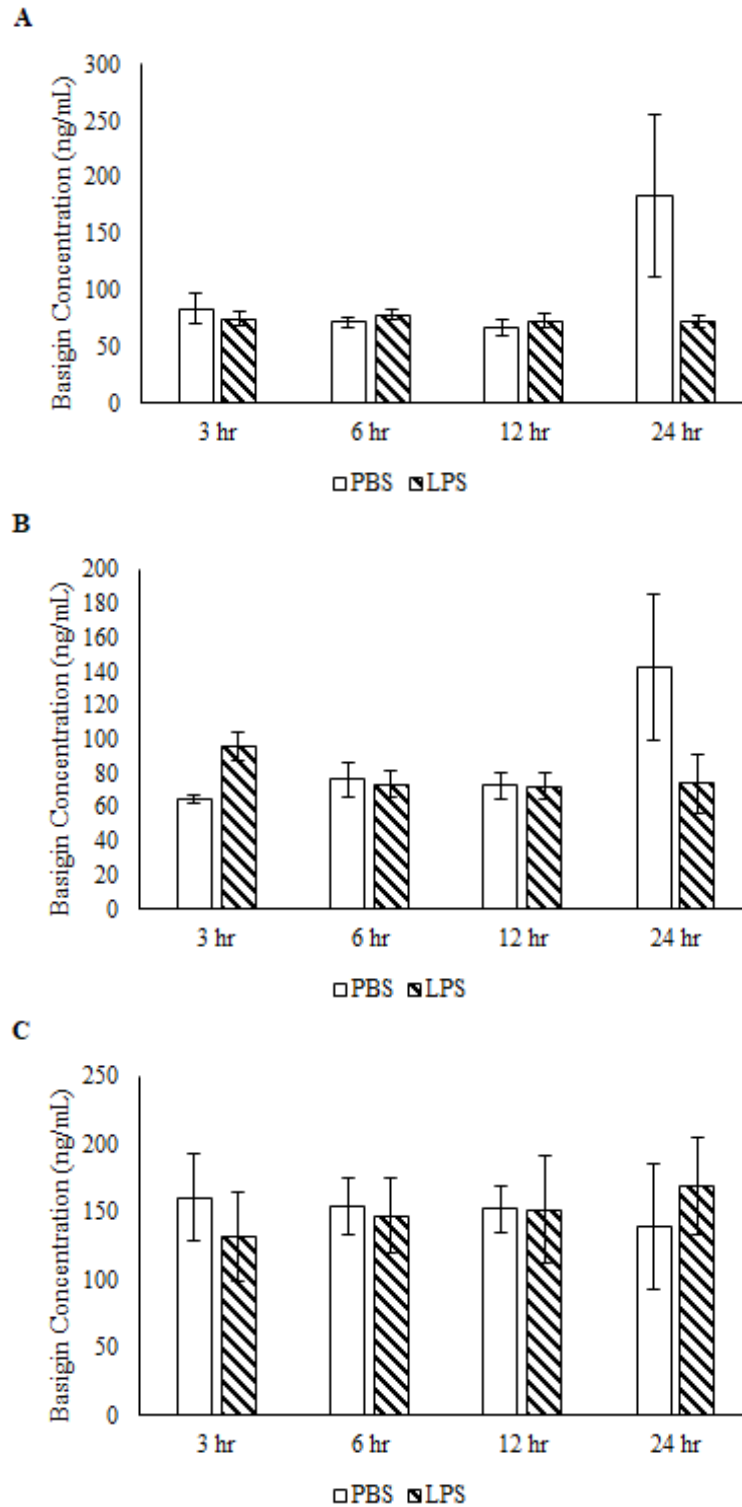


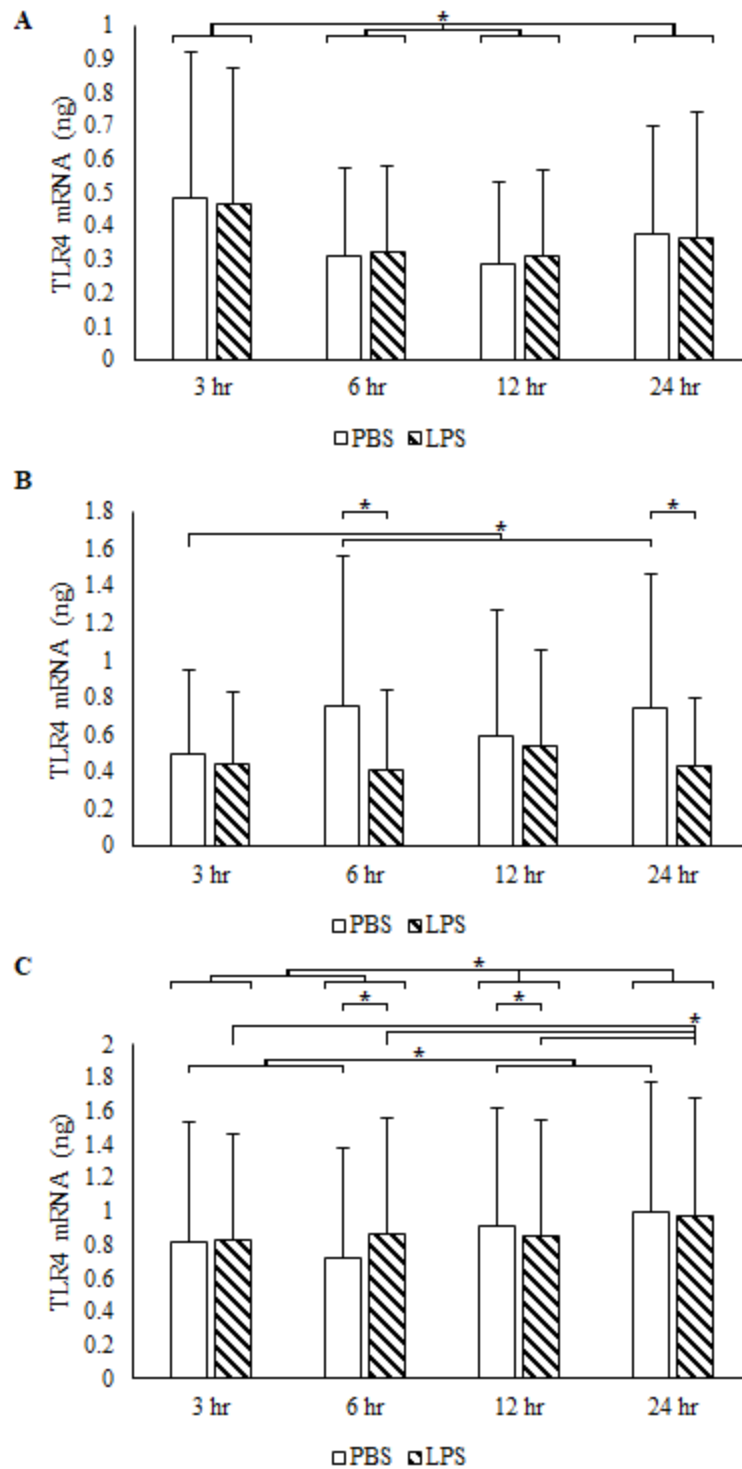
**Figure 2.2 Quantitative analyses of Basigin protein in neonate, adolescent, and adult mice.** A direct ELISA for Basigin protein expression was performed using protein isolated from brain tissue incubated in DMEM  $\pm$  LPS for 3, 6, 12, or 24 hours of mice at PD 7 (A), PD 30 (B), and PD 180 (C). White bars represent tissue incubated with PBS as a control, while dashed bars represent tissue incubated in LPS. The runs were performed in duplicate. Error bars represent the standard error.

### **Expression of TLR4**

To determine whether TLR4 transcript expression was similar to that of Basigin, TLR4 mRNA was quantified. In mice at PD 7 the highest amount of TLR4 transcripts were quantified in tissues incubated for 3 hours (Figure 2.3A). A significant decrease was observed at the 6-hour time point, followed by an upregulation in transcript levels after 24 hours. The time for which the tissues were incubated showed a significant main effect on the expression of TLR4 ( $p = 3.05 \times 10^{-8}$ ). The Treatment did not have an observable main effect on TLR4 expression ( $p = 0.861$ ), nor was there a significant interaction effect within this age group ( $p = 0.466$ ).

Mice at PD 30 displayed a different pattern of TLR4 expression than those at PD 7 (Figure 2.3B). After 3 hours of incubation, PBS treated tissue expressed less TLR4 when compared to 6- and 24-hour incubated tissue within the same treatment group. The 6- and 24-hour PBS treated tissue also expressed a greater amount of TLR4 transcripts when compared to LPS treated tissue of the same incubation periods. Incubation time did not have as much of an effect ( $p = 0.053$ ), as tissues incubated for 6 hours had only a slight increase in TLR4 transcript levels. However, treatment was determined to have a significant main effect ( $p = 2.81 \times 10^{-5}$ ). On average, tissues incubated in LPS expressed significantly less TLR4 than those incubated in PBS. Additionally, a significant interaction effect was observed ( $p = 6.69 \times 10^{-3}$ ).

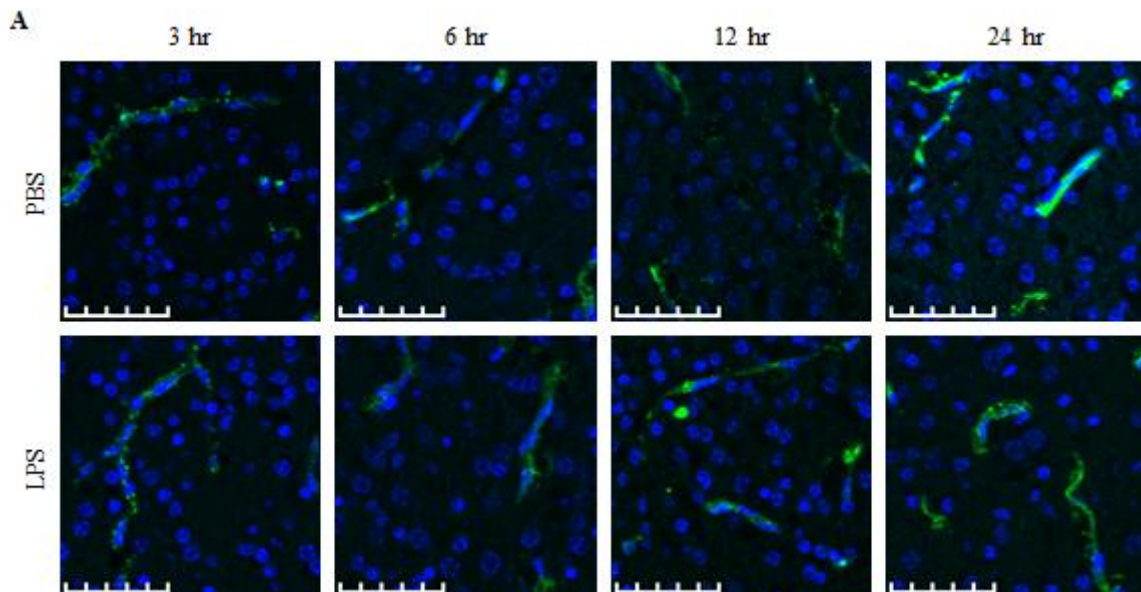
Quantification of TLR4 mRNA of mice at PD 180 revealed that TLR4 expression did not change between the 3- and 6-hour incubation period, but steadily increased thereafter (Figure 2.3C). In PBS treated tissue, TLR4 increased in expression from the 6- to 12-hour time point, while in LPS treated tissue, TLR4 did not significantly increase until the 24-hour incubation period. Incubation time had a significant effect ( $p = 3.14 \times 10^{-8}$ ), regardless of treatment. Treatment did not have an observable main effect ( $p = 0.204$ ), but a significant interaction effect was found ( $p = 8.55 \times 10^{-5}$ ).

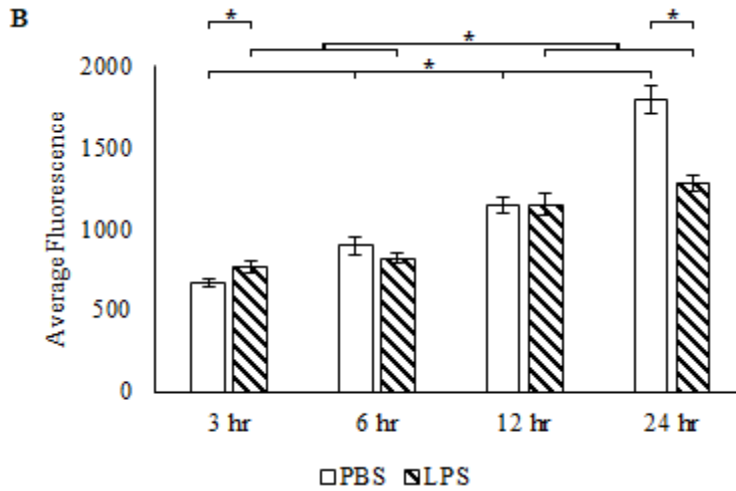


**Figure 2.3 Quantitative analyses of TLR4 transcripts in neonate, adolescent, and adult mice.** Quantitative reverse transcription PCR was performed on RNA isolated from brain tissue incubated in DMEM  $\pm$  LPS for 3, 6, 12, or 24 hours of mice at PD 7 (A) and PD 30 (B), using primers complementary to TLR4. White bars represent tissue incubated with PBS as a control, while dashed bars represent tissue incubated in LPS. Error bars represent the coefficient of variation. \* indicates a p-value  $<$  0.05 by Tukey's HSD test, following a two-way ANOVA.

## Localization

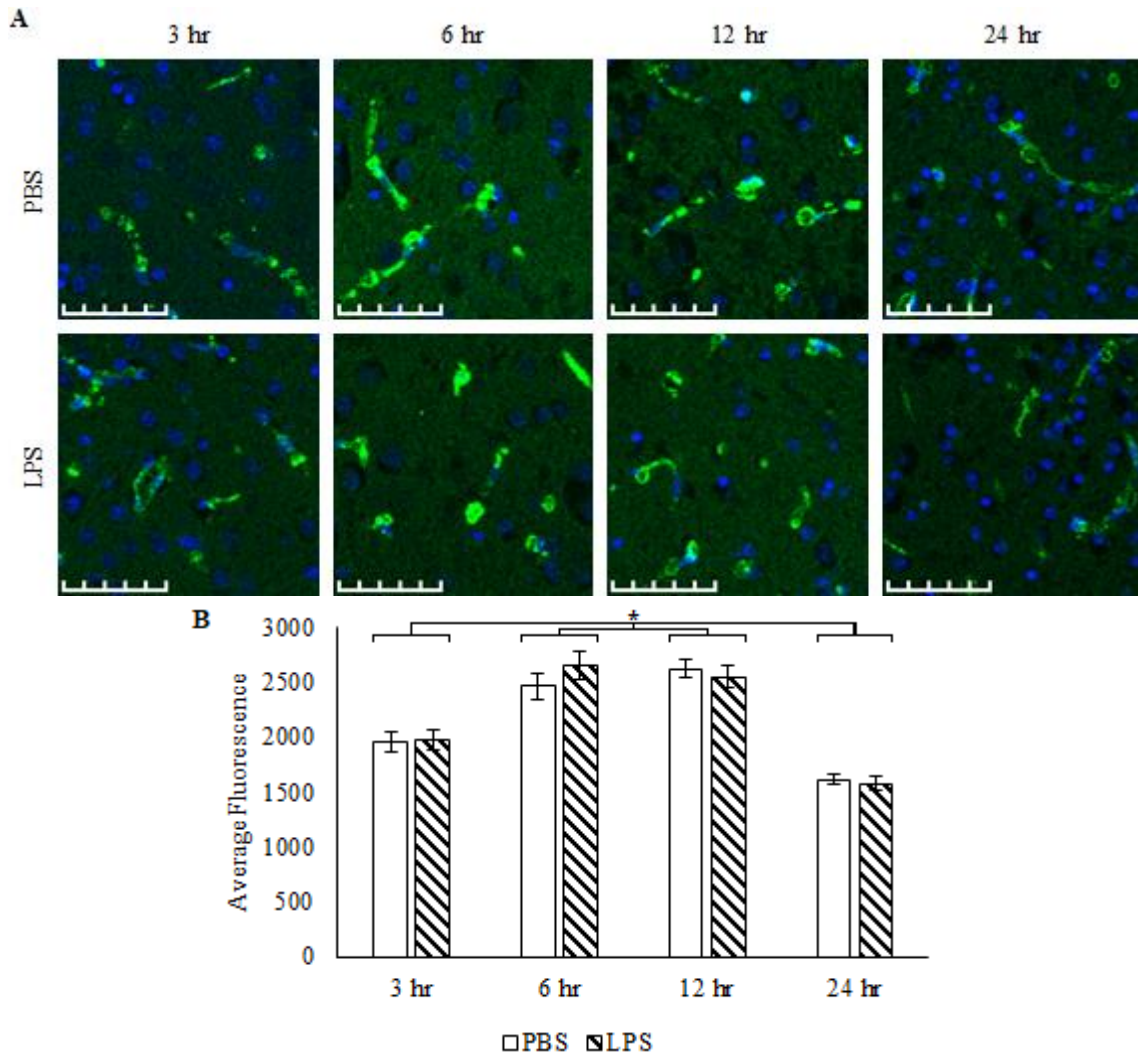
Immunohistochemical analyses were performed to localize and quantify the expression of Basigin within mouse brain tissue sections. In mice at PD 7, the antibody that recognizes Basigin produced a signal on microvascular endothelial cells (Figure 2.4A). Comparing the average fluorescence of 20 regions of interest (ROIs) taken from each treatment group per time point revealed that although, on average, tissue treated with LPS expressed significantly less Basigin than tissue incubated with PBS ( $p = 0.002$ ), Basigin expression significantly increased in tissues of both treatment groups as incubation time increased ( $p = 1.7 \times 10^{-34}$ ; (Figure 2.4B). Further, a significant interaction effect was also observed ( $p = 1.03 \times 10^{-7}$ ). Basigin expression significantly increased in tissues incubated with PBS for each time period, while only significantly increasing from hour 6 to 12 within the group of brain tissues treated with LPS. Basigin expression was significantly higher in brains treated with LPS when incubated for 3 hours, but significantly lower when incubated for 24 hours, compared to those treated with PBS.





**Figure 2.4 Localization and quantification of Basigin in PD 7 mouse brain tissue.** (A) Immunohistochemistry was performed on brain tissue sections of mice at PD 7 to localize the expression of Basigin (green). DAPI was used to stain nuclei (blue). Magnification bar, 50  $\mu\text{m}$ . (B) Quantification of the average fluorescence for each treatment is shown as a bar graph. White bars represent tissue incubated with PBS as a control, while dashed bars represent tissue incubated in LPS. Error bars represent standard error. \* indicate a p-value < 0.05 via a two-way ANOVA followed by a Tukey's HSD test.

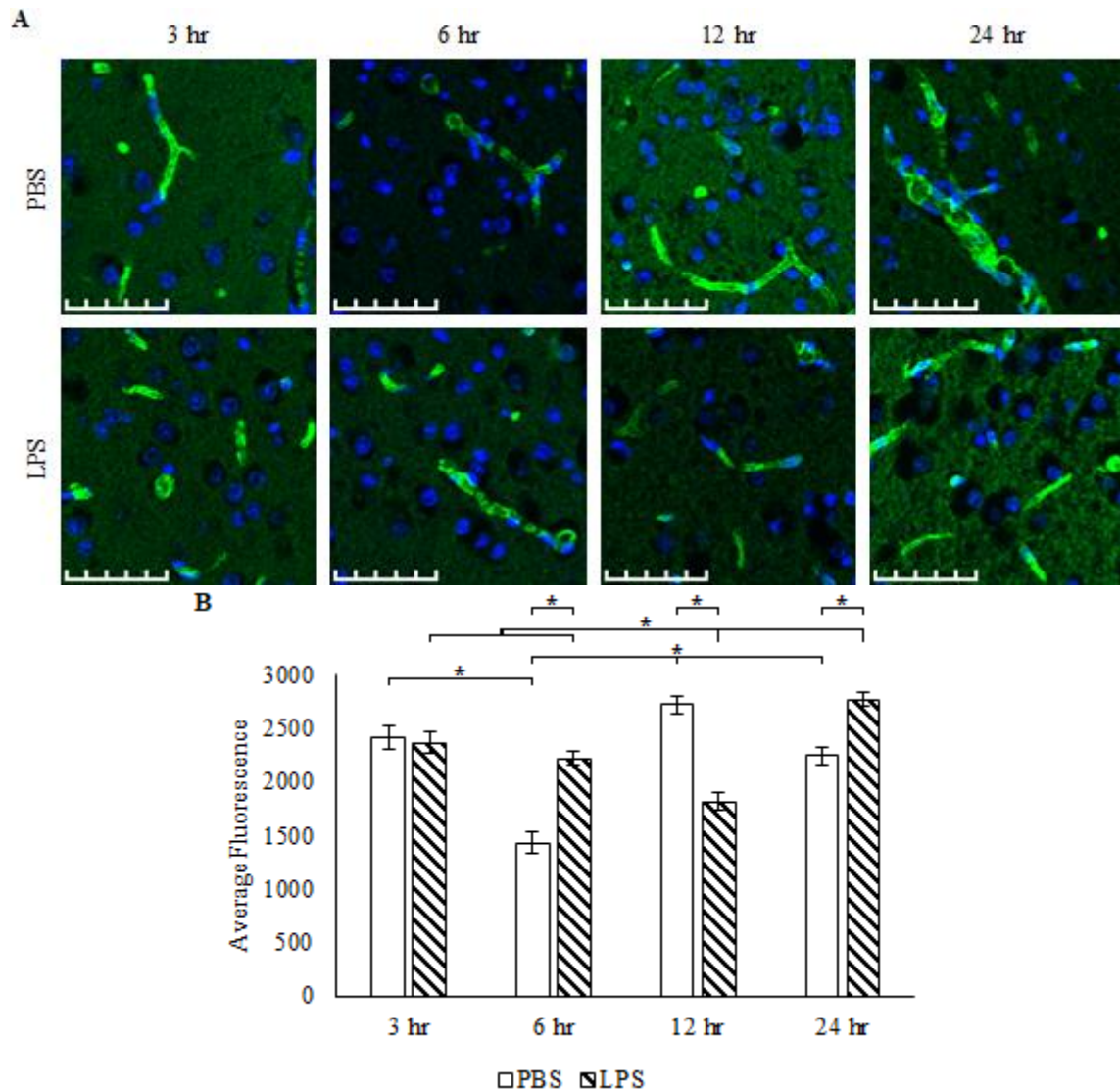
Basigin expression was localized to the microvasculature in mice at PD 30, like that of mice at PD 7 (Figure 2.5A). However, the average fluorescence emitted differed (Figure 2.5B). Brain tissue incubated for 6 and 12 hours expressed significantly more Basigin than those incubated for 3 and 24 hours, regardless of treatment. Treatment did not have an observable main effect ( $p = 0.677$ ), but time in which tissues were incubated did ( $p = 8.74 \times 10^{-24}$ ). No significant interaction effect was observed ( $p = 0.491$ ).



**Figure 2.5 Localization and quantification of Basigin in PD 30 mouse brain tissue. (A)** Immunohistochemistry was performed on brain tissue sections of mice at PD 30 to localize the expression of Basigin (green). DAPI was used to stain nuclei (blue). Magnification bar, 50  $\mu$ m. **(B)** Quantification of the average fluorescence for each treatment is shown as a bar graph. White bars represent tissue incubated with PBS as a control, while dashed bars represent tissue incubated in LPS. Error bars represent standard error. \* indicate a p-value < 0.05 via a two-way ANOVA followed by a Tukey's HSD test.

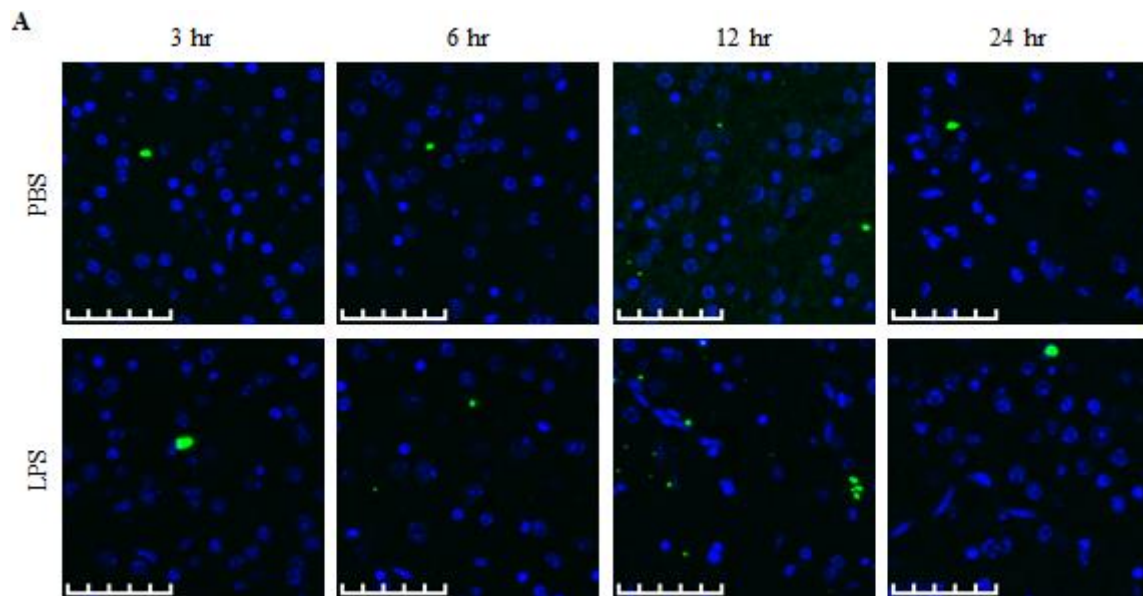
In mice at PD 180, the localization of signal produced from immunostaining had a similar profile to that of mice at PD 7. The fluorescence was concentrated around the brain's microvasculature (Figure 2.6A). Upon analysis of the average fluorescence emitted, it was determined that Basigin expression for brains incubated in PBS fluctuated significantly beginning at 6 hours to 24 hours. Brain tissue incubated in LPS also showed a fluctuation in

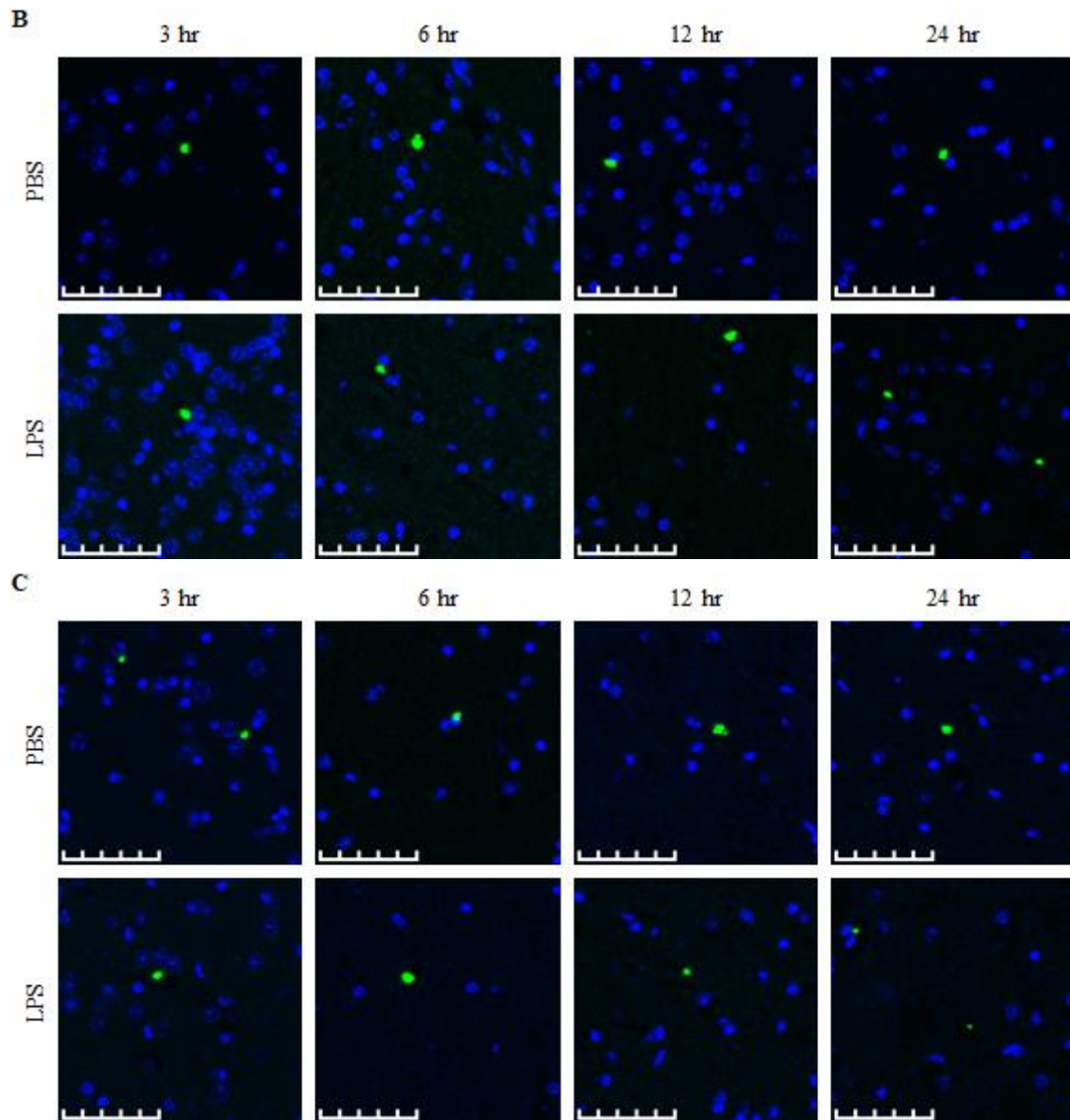
Basigin expression but was inverse to that of PBS-incubated tissue. That is, LPS treatment of tissues incubated for 6 and 24 hours expressed significantly more Basigin than tissues incubated with PBS but expressed significantly less at the 12-hour timepoint (Figure 2.6B), Treatment did not have an observable main effect ( $p = 0.147$ ), while incubation period did ( $p = 1.2 \times 10^{-12}$ ; Figure 2.6B). Further, a significant interaction effect was observed within this age group ( $p = 2.95 \times 10^{-18}$ ).



**Figure 2.6 Localization and quantification of Basigin in PD 180 mouse brain tissue.** (A) Immunohistochemistry was performed on brain tissue sections of mice at PD 180 to localize the expression of Basigin (green). DAPI was used to stain nuclei (blue). Magnification bar, 50  $\mu\text{m}$ . (B) Quantification of the average fluorescence for each treatment is shown as a bar graph. White bars represent tissue incubated with PBS as a control, while dashed bars represent tissue incubated in LPS. Error bars represent standard error. \* indicate a p-value < 0.05 via two-way ANOVA followed by a Tukey's HSD test.

A previous study by this laboratory suggested that the Basigin-TLR4 interaction is stabilized through both hydrophilic and hydrophobic interactions, *in vitro*.<sup>34</sup> To determine whether this interaction occurs *ex vivo* when presented with an inflammatory stimulus, an immunohistochemical analysis of TLR4 was performed on the same tissues that underwent treatment as described above. The signal produced by an antibody specific to TLR4 demonstrated sparse distribution of the protein within the tissue at all ages and was not consistent with the immunohistochemistry of Basigin (Figure 2.7). Distribution changes due to treatment incubation were not quantified, but there appeared to be no change in the expression of TLR4 across all tissues.

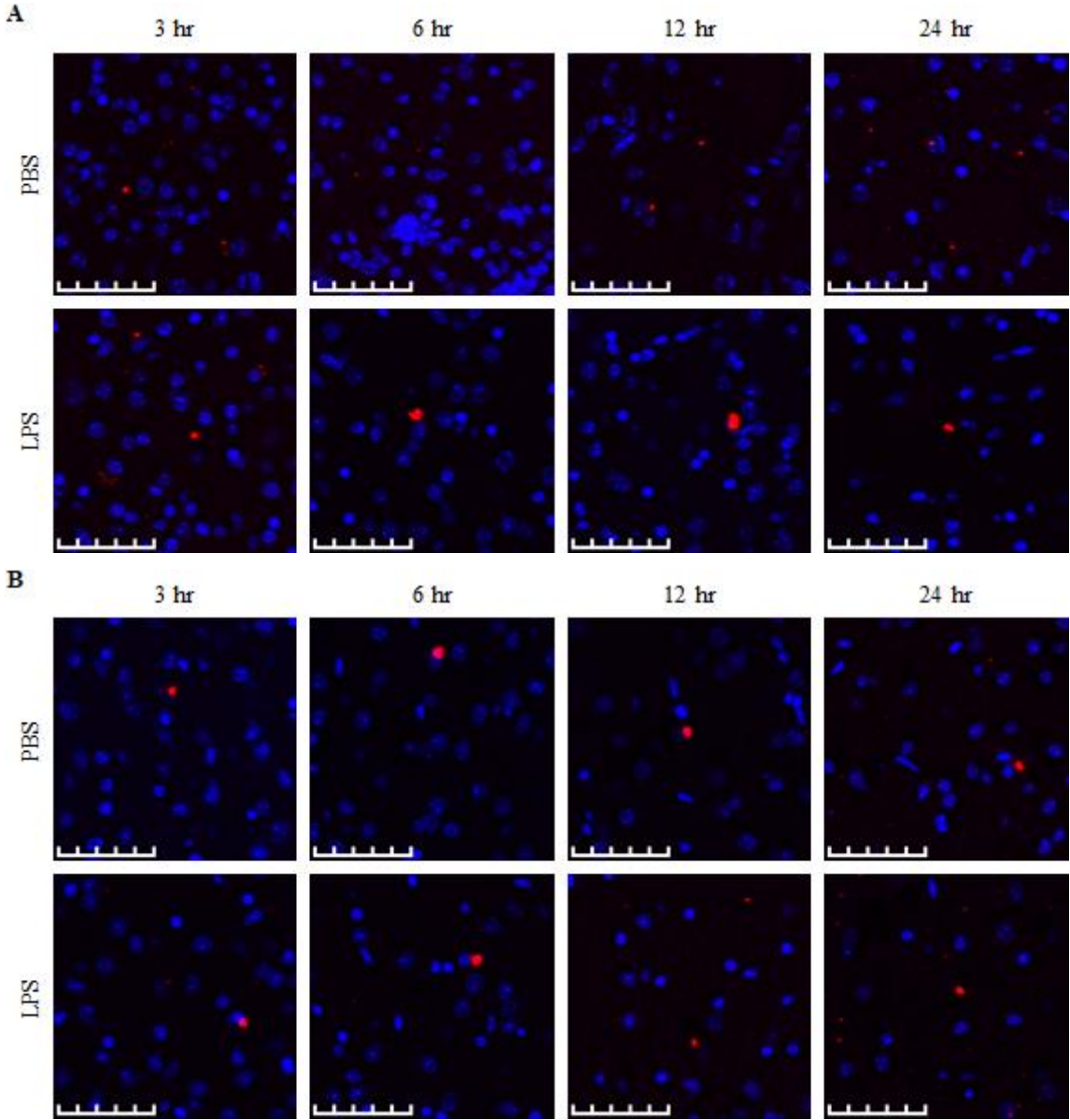




**Figure 2.7 Localization of TLR4 in neonate, adolescent, and adult mouse brain tissue.** Immunohistochemistry was performed on brain tissue sections of mice at PD 7 (A), PD 30 (B), and PD 180 (C) to localize the expression of TLR4. The staining of TLR4 is shown in green (AF-488) was distributed sparingly within the tissue. DAPI (blue) was used to stain nuclei. Magnification bar, 50  $\mu$ m.

To further investigate the hypothesis that Basigin may play a role in mediating an inflammatory response through TLR4, immunohistochemistry was used to localize the expression of the cytokine, IL-6. In mice, IL-6 production was like that of TLR4, rather than

Basigin and did not increase with incubation time in either treatment group across all ages (Figure 2.8).



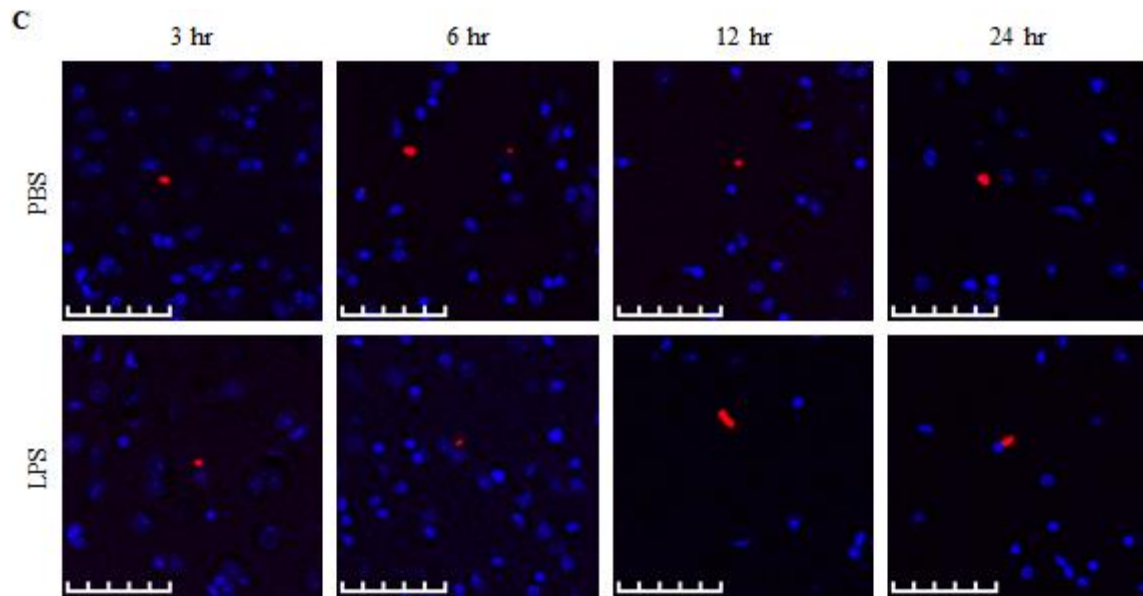


**Figure 2.8 Localization of IL-6 in neonate, adolescent, and adult mouse brain tissue.** Immunohistochemistry was performed on brain tissue sections of mice at PD 7 (A), PD 30 (B), and PD 180 (C) to localize the expression of IL-6. The distribution of IL-6 (pseudo colored red, AF-488) was not found in abundance. DAPI (blue) was used to stain nuclei. Magnification bar, 50  $\mu\text{m}$ .

## Discussion

Basigin is a widely distributed gene product that has diverse function, dependent on its expression within the tissue and cell type. Basigin's association with MCTs and GLUT proteins have been illustrated as essential for spermatozoa<sup>88</sup>, photoreceptor cells<sup>33,89</sup> and neurons.<sup>90</sup> However, Basigin has also been implicated in pathogen recognition, infiltration, and cytokine production.<sup>91,92</sup> Further, Basigin is upregulated in activated human vein endothelial cells and spurs angiogenesis.<sup>93</sup> Considering endothelial cells are an integral component of the BCB, this study aimed to characterize Basigin expression in brain endothelium when exposed to an inflammatory stimulus for a varying degree of time in neonatal, adolescent, and adult mice.

Immunohistochemical techniques indicated that Basigin is indeed expressed on blood vessels in mice within all age and treatment groups. Quantification of the average fluorescence revealed that in the neonatal (PD 7) brain, Basigin expression steadily increased from 3 to 24

hours, post dissection, without the addition of LPS. However, LPS induced an increase in Basigin expression only from the 6- to 12-hour incubation period. The continuous upregulation of Basigin in PBS treated tissue could be a result of the hypoxic condition the tissue was under, as it has been suggested an upregulation of the Basigin-MCT4 complex under hypoxic conditions may be a means of adaptation.<sup>94</sup> Interestingly, the addition of an inflammatory stimulus suppressed the degree to which Basigin was upregulated in the long-term.

The analysis of Basigin transcripts in neonatal brain tissue indicated transcription occurred most abundantly during the first 3 hours of incubation in both treatment groups. A steep decline in the rate of transcription occurred at the 6-hour time point and did not recover for the remainder of the time in which the tissue was incubated. These data taken with the immunohistochemical data suggest either a delay in protein synthesis<sup>95</sup>, or a delay in the degradation of the protein synthesized.<sup>96</sup> The copious amounts of Basigin transcripts in the 3-hour incubated tissue is potentially due to the change in nutrient environment. Additionally, these data may differ from that of those obtained via immunohistochemical techniques due to a small sample used from a homogenous pool of half the brain tissue, rather than from one section of brain tissue.

In an effort to quantify the amount of Basigin protein within the brain, direct ELISAs were performed. The analyses of the assay indicated no change in Basigin expression during any incubation period or within treatment groups at PD 7. As it was revealed that Basigin is highly localized to brain vasculature, the limited concentration of Basigin in relation to all other protein within brain tissue could account for the negligible shifts in concentration.

Although immunohistochemistry of adolescent (PD 30) brain tissue also indicated Basigin to be highly localized to blood vessels, the pattern in expression of Basigin after varying

degrees of incubation with LPS varied from neonatal brain tissue. The increase in Basigin expression in either treatment group was marginal as incubation time reached 12 hours. However, a steep decline in expression at the 24-hour time point of both treatment groups indicates the inflammatory stimulus is not the cause in downregulation. Further, the lack of variance in tissues incubated with LPS compared to those without suggests this age group is more resilient to an inflammatory stressor.

Transcript and protein analyses of Basigin in adolescent mice indicated similar trends in expression as neonatal mice, in that transcript levels were the most abundant during the 3-hour incubation period, though the transcript abundance was maintained into the 6-hour time point. The sustained level of transcripts and no change in protein expression among treatment groups support the notion that adolescent mice are less susceptible to pathogenic disturbance.

Basigin expression in the adult (PD 180) brain differed from the other age groups in immunohistochemical and transcriptional analyses. The quantification of the average fluorescence, localized to blood vessels, determined a fluctuation in Basigin expression in PBS treated mice. That is, a decrease in expression was observed from 3 to 6 hours of incubation, followed by a recovery at 12 hours and a slight decline at 24 hours. Conversely, LPS induced a steady decline in Basigin expression from 3 to 12 hours, followed by an increase at 24 hours. These data suggest LPS alters the regulation of Basigin in the adult brain.

Though transcript analyses for this age group determined a steady decline in Basigin transcripts from 3 to 12 hours, with a slight recovery after 24 hours, these shifts were negligible in comparison to transcript levels in neonatal and adolescent brain tissue. Further, the trends observed in Basigin transcription did not mirror what was observed in immunohistochemical analysis.

TLR4 is a well characterized recognition receptor of LPS.<sup>6</sup> A previous study, by this laboratory, has demonstrated TLR4's association with Basigin, *in vitro*.<sup>34</sup> Therefore, we sought to quantify the level of transcripts and localize the protein in brain tissue in the presence of LPS. In neonatal mice, TLR4 transcription is similar to Basigin transcription at this age, in that the highest expression was quantified at the 3-hour incubation period, with a decline at 6 hours. Unlike Basigin transcripts, TLR4 recovered at the 24-hour time point. No difference of expression among treatment groups was observed, suggesting the regulation of TLR4 was not influenced by LPS at this age.

In adolescent mice, TLR4 expression notably increased from the 3- to 6-hour incubation period in tissues treated with PBS, but not with LPS. Further, transcript levels were considerably lower in LPS treated tissue at the 6- and 24-hour time point, compared to control, indicating a suppressive regulatory effect of LPS on TLR4 upon specific degrees of exposure.

The most notable differences in TLR4 expression was observed in adult brain tissue. In control tissue, an increase in TLR4 transcripts was observed from the 6- to 12-hour incubation period and maintained through 24 hours. While in tissues incubated with LPS, the increase in expression was observed at the 24-hour incubation period. Additionally, TLR4 expression was higher in LPS treated tissue at the 6-hour time point, but lower at the 12-hour time point, compared to control. This is indicative of the potential influence LPS has on the regulation of TLR4. The variability in response seen, dependent on age, suggests pathogen susceptibility increases as age increases.

Immunohistochemical analyses of TLR4 did not mirror the transcript analyses. The localization of TLR4 was sparse in all age groups across all incubation periods and did not appear to vary. Additionally, no labeling of the blood vessels was observed. These data are not

consistent with the literature, as a previous study demonstrated TLR4 was expressed on endothelial cells and upregulated in response to LPS.<sup>97</sup> The inconsistency in our findings could be due to a masking of the epitope recognized by the antibody used in this experiment.

The activation of TLR4 by LPS initiates the production of IL-6.<sup>16-20</sup> Therefore, IL-6 expression was characterized by immunohistochemistry in brain tissue stimulated with LPS. The analyses indicated a distribution much like that of TLR4. Labeling of IL-6 was sparse in all age groups and among treatment groups, with very little change across all samples. The lack of variation between treatment groups could be due to the release of IL-6 in the media, rather than sequestered to the tissue. Given that no shift in labeling of TLR4 was observed, it is also possible that TLR4 was not activated, thus no IL-6 was produced.

The results herein conclude Basigin is highly expressed on blood vessels within the mouse brain. The exposure to LPS affected the level of expression in a time-dependent manner, but not in the same way at each age. The change in expression in neonates and adults, but not in adolescent mice, suggests the former age groups are more vulnerable to an inflammatory stressor, and perhaps more susceptible to peripheral infiltration. The unmatched pattern of expression between Basigin and TLR4 suggest these gene products are not regulated in the same manner. It is possible Basigin's role in inflammation is not to associate with TLR4, but potentially CD44, a lymphocyte homing receptor implicated in angiogenesis.<sup>98</sup>

The localization of Basigin to endothelial cells partially confirmed our hypothesis based on the findings from the Fryer Laboratory at the Mayo Clinic Florida. However, our findings differed in that we did not see a two-fold increase in Basigin expression after long-term exposure to LPS. These differences could be due to way in which each experiment was conducted. The Fryer Laboratory delivered LPS in-vivo and subsequently isolated RNA immediately after

dissection. Although the 18S rRNA data did not indicate degradation of the tissue used in this experiment, other unknown factors could have contributed to the observed effects.

### **Chapter 3 – The influence of LPS on Basigin and TLR4 Transcription in the Retina**

In 2018, the Center for Disease Control and Prevention estimated that 10.5% of Americans had diabetes mellitus. Patients who suffer from diabetes mellitus often also develop diabetic retinopathy (DR).<sup>99</sup> The first stage of DR is known as non-proliferating and is marked by damage to retinal vasculature, increased vascular permeability, and loss of pericytes.<sup>100</sup> As the pathology progresses into the proliferating stage, angiogenesis, vitreous hemorrhaging, and tractional retinal detachment occurs, resulting in vision loss.<sup>101</sup> Diabetic macular edema (DME) is an occurrence of both DR stages in which vascular permeability and protein leakage increases. The increase in extracellular fluid is collected by Müller cells, resulting in swelling and death of Müller cells, exacerbating vision loss.<sup>102,103</sup>

During embryonic development bilateral optic vesicles are formed by the evagination of the ventral forebrain neuroepithelium.<sup>104</sup> The distal portion of the vesicle interacts with the lens ectoderm, resulting in invagination and the formation of a bilayered optic cup. Because the retina develops from the layer of the optic cup originating from the diencephalon, it is considered to be part of the central nervous system (CNS).<sup>105</sup> The neural retina can be divided into ten layers consisting of various cell types, including photoreceptor cells, Müller cells, and endothelial cells. The arrangement of these cell layers allows for proper light transmission, but may also leave the retina susceptible to developing DR. For instance, the low distribution of blood vessels is necessary for proper light transmission, as they absorb light and interfere with retinal function. Consequently, there is a low distribution of oxygen, with a decline in partial pressure in the distal retina.<sup>106</sup>

Photoreceptor cells demand high amounts of oxygen and glucose for proper function. The majority of these necessary nutrients are provided by the choroid vasculature, which lies

proximal to the retinal pigmented epithelium (RPE).<sup>107</sup> Tight junctions between retinal epithelial cells form the outer blood-retinal barrier (BRB), which regulates solute and nutrient movement from the choroid to the sub-retinal space.<sup>108</sup> Epithelial, choroidal and Müller cells, along with the outer segments of photoreceptor cells, express glucose transporter 1 (GLUT1) to facilitate the passive movement of glucose for metabolism by photoreceptors.<sup>109,110</sup> Glucose is transported from photoreceptor cells to Müller cells via GLUT1 and metabolized to lactate for use in anaerobic glycolysis.<sup>111</sup> Excess lactate is shuttled out of the retina by a family of proton-coupled monocarboxylate transporters (MCTs), expressed on the same cells. The lactate shuttled to photoreceptors can also be used to fuel oxidative phosphorylation.<sup>30</sup>

It has been proposed that a lactate metabolon is formed by the interaction of MCTs and Basigin gene products.<sup>33,112</sup> The Basigin gene expresses two glycoprotein isoforms, Basigin-variant-1 (B-v1) and Basigin-variant-2 (B-v2).<sup>24</sup> Both gene products are members of the immunoglobulin super family (IgSF) and are identical in amino acid sequence, except for the extra immunoglobulin domain expressed by B-v1. B-v1 is specifically expressed by photoreceptor cells, while B-v2 has a wide distribution within many tissues and highly expressed on endothelial cells.<sup>24</sup> The expression of Basigin gene products in the retina is critical for proper development, as demonstrated by complete blindness and subsequent retinal degeneration in Basigin null mice.<sup>113,114</sup> Though necessary for the developing retina, B-v2 induces the production of matrix metalloproteinases, and vascular endothelial growth factor, spurring angiogenesis.<sup>26</sup> Further, studies by this laboratory have demonstrated B-v2 interacts with Toll-like receptor 4 (TLR4), potentially promoting an inflammatory response.<sup>34</sup>

As the progression of DR is marked with chronic inflammation, this study aimed to address the potential role Basigin gene products play in retinal pathogenesis by way of its

association to TLR4. TLR4 is a well characterized recognition receptor of the endotoxin, LPS. Thus, the purpose of the present study was to quantify Basigin gene and TLR4 transcripts in the neural retina after varying degrees of exposure to LPS. Further, the dynamics of expression due to age were characterized.

## **Materials and Methods**

### **Animals**

All experiments described in the present study were approved by the University of North Florida Institutional Animal Care and Use Committee (IACUC) under protocols #17-003 and #19-008 and were conducted in accordance with the American Veterinary Medicine Association (AVMA). Mice were housed at the University of North Florida vivarium in accordance with institutional requirements for animal care and were maintained under a standard 12:12 h light/dark cycle and were allowed *ad libitum* access to 8604 Harlan Teklad Rodent Chow (Harlan Research Models and Services, Indianapolis, IN) and water.

### **Treatment of Tissue**

Eyes were dissected from female and male wild-type C57/129 hybrid mice<sup>87</sup> at postnatal days (PD) 7, 30, and 180. Three pairs of eyes were dissected per age group and incubated in DMEM + PBS or LPS (10 µg/mL; InvivoGen, San Diego, CA) at 37°C with 5% CO<sub>2</sub> for 3, 6, 12, or 24 hours. Following incubation, retinal tissue from one eye per animal was dissected and directly frozen at -80°C, while the other eye was preserved by immersion-fixation in 4% paraformaldehyde in phosphate-buffered saline for 24 hours at 4°C, followed by incubation in 100% ethanol at -20°C.

### **cDNA Isolation**

cDNA was produced without RNA isolation from dissected retinal tissue using the Cells-to-cDNA™ II Kit (Thermo Fisher Scientific Inc., Waltham, Massachusetts). Retinal tissue was first washed with 100 µL of PBS (pH 7.4), then homogenized in 100 µL of Cell Lysis II Buffer. The homogenized solution was incubated at 75°C for 10 minutes, followed by an addition of 2 µL of DNase I, and a subsequent incubation at 37°C for 15 minutes. Inactivation of the DNase was achieved by incubating the tissue homogenate at 75°C for 5 minutes. A 5 µL sample of the homogenate was combined with 4 µL dNTP mix and 2 µL of Oligo(dT)<sub>18</sub> primer, then incubated for 3 minutes at 70°C. Finally, 2 µL of RT buffer, 1 µL of M-MLV reverse transcriptase, and 1 µL of RNase inhibitor was added to the reaction mixture and incubated at 42°C for 1 hour then 92°C for 10 minutes.

### **Quantification of Basigin and TLR4 mRNA Expression**

The isolated cDNA was used to quantify the expression of both Basigin gene products and TLR4 in retinal tissue of mice at PDs 7, 30, and 180. Amplification of cDNA was detected using a nucleic acid fluorogenic dye (SYBR Green; iUniversal, Bio-Rad, Inc.) and primers complementary in sequence to the cDNA of B-v1, B-v2, TLR4 and mouse 18S ribosomal RNA. The primer sequences used are as follows: B-v1 Fwd 5' – TGGACCGTGTTCCATCCAT; B-v1 Rvs 5' – CCCATC-AACAGAGAGCGAACT; B-v2 Fwd 5' – CTGCGCGGCGGCGGGCAC-CAT; B-v2 Rvs 5' – GCTGTTCAAAGAGCAGGTAAGCT; TLR4 Fwd 5' – CACCGTGATTG-TGGTATCCACTGT; TLR4 Rvs 5' – GTCCTCATTCTGACTCGAGTAGAT; 18S Fwd 5' – AGTCCCTGCCCTTTGTACACA; 18S Rvs 5' – CCGAGGGCCTCACTAAACC. Although Basigin and 18S sequences were already established<sup>24</sup>, the primer sequence complimentary to TLR4 was designed using NCBI's Primer-

BLAST software in conjunction with the GenBank TLR4 sequence (accession: NM\_021297.3). All runs were performed in triplicate using a CFX Connect Real-Time PCR Detection System (Bio-Rad, Inc.) and used standard melt curve analyses. Thermal cycling protocols were set according to the manufacturer. The amount of each amplified product was calculated using a standard curve generated for each primer set. Expression of Basigin and TLR4 were normalized to 18S ribosomal RNA expression. The square root of each gene product was taken prior to analyses by a two-way ANOVA and subsequent Tukey's HSD test, to ensure normality of the data.

## **Results**

### **Expression of Basigin Gene Products and TLR4**

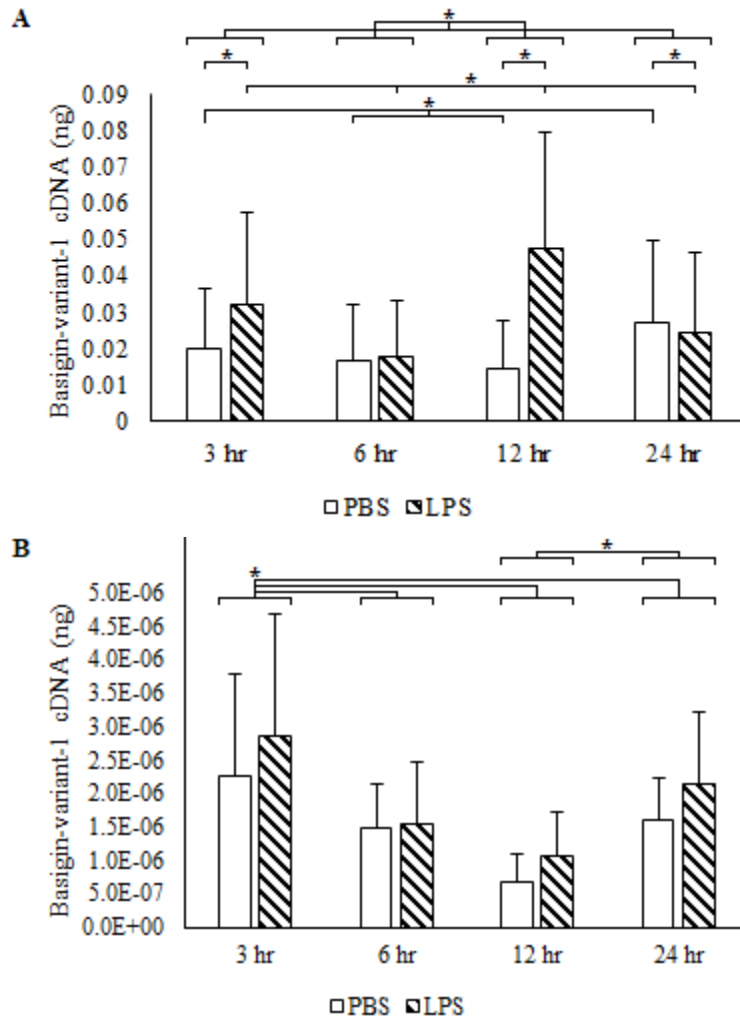
To quantify the expression of Basigin gene products in the neural retina in response to a well characterized endotoxin, LPS, cDNA isolated from mice at PDs 7, 30, and 180 was analyzed. In PD 7 mice, the average B-v1 expressed in tissue incubated with LPS was higher than that of tissue incubated in PBS ( $p = 2.3 \times 10^{-14}$ , Figure 3.1A). Tissues incubated for 12 hours yielded the highest expression of B-v1 transcripts, while tissues incubated for 6 hours yielded the lowest, regardless of treatment. In tissues incubated with PBS, a decline in B-v1 expression was observed from the 3- to 6-hour time point, followed by nearly a two-fold increase at the 24-hour time point. Treatment of LPS induced an increase in B-v1 expression during the 3-hour incubation period, compared to PBS. This was followed by a notable decline at the 6-hour time point, returning expression back to control. At the 12-hour incubation period, LPS induced another spike in B-v1 transcripts, followed by another decline after 24 hours.

The time which the tissues were incubated had an effect on the quantity of B-v1 transcripts produced ( $p = 1.6 \times 10^{-12}$ ). Further, a significant interaction effect was observed ( $p = 7.6 \times 10^{-15}$ ).

B-v1 expression in retinal tissue of mice at PD 30 did not resemble that of PD 7 mice (Figure 3.1B). While the tissue incubated in LPS also expressed more B-v1, on average, than PBS-treated tissue ( $p = 0.02$ ), the incubation periods affected expression differently ( $p = 2.1 \times 10^{-5}$ ). Retinal tissue incubated for 3 hours expressed significantly more B-v1 compared to all other time points. A significant increase in expression was also observed from the 12- to 24-hour incubation period, regardless of treatment. No significant interaction effect was observed ( $p = 0.6$ ).

Though significant differences in B-v1 expression was observed in mice at PD 180, these differences did not follow the same trend as the other age groups (Figure 3.1C). After 3 hours post-treatment, B-v1 expression was the most abundant. It then significantly declined at 6 hours and did not significantly increase again until the 24-hour incubation period. On average, B-v1 expression was greater in retinal tissue incubated in PBS ( $p = 1.6 \times 10^{-8}$ ). The time in which the tissue was incubated also affected the amount of B-v1 expressed ( $p = 2.4 \times 10^{-10}$ ). A significant interaction effect was observed ( $p = 2.1 \times 10^{-12}$ ). The trend of B-v1 expression in PBS treated tissue was similar to that of the effect seen for incubation time. B-v1 expression was highest at 3 hours, declined at 6 hours, and did not significantly increase again until the 24-hour time point. Tissues incubated with LPS fluctuated throughout the duration of the experiment. A significant decline in expression was observed from 3 to 6 hours of incubation, followed by a spike at 12 hours and another decline after 24 hours. Compared to PBS treated tissue, those treated with LPS

expressed lower B-v1 transcripts at the 3- and 24-hour time point, but more at the 12-hour time point.



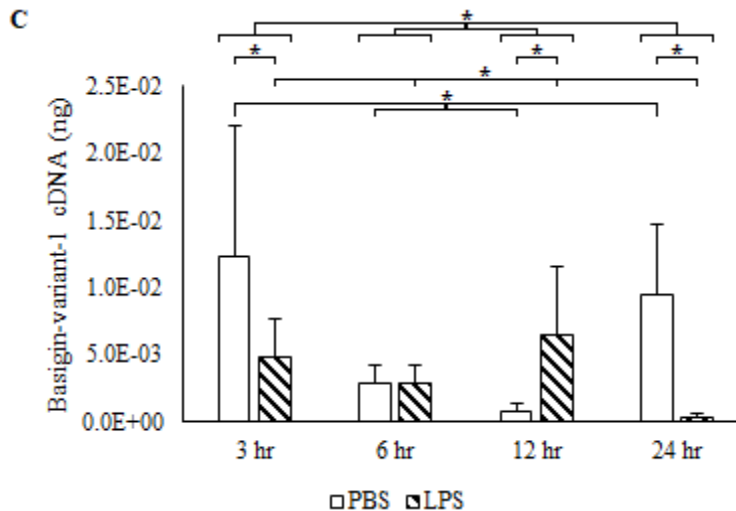
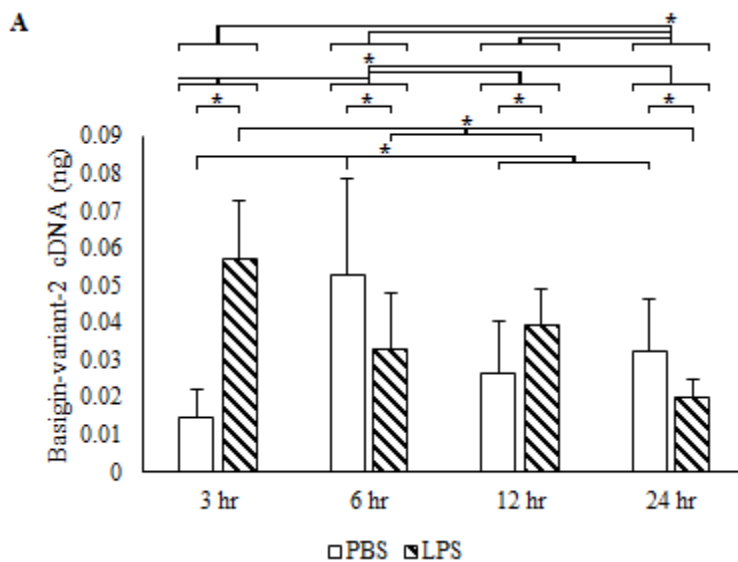


**Figure 3.1 Quantitative analyses of Basigin-variant-1 transcripts in neonate, adolescent, and adult mice.** Quantitative PCR was performed on cDNA isolated from retinal tissue incubated in DMEM  $\pm$  LPS for 3, 6, 12, or 24 hours of mice at PD 7 (A), PD 30 (B) and PD 180 (C), using primers complementary to B-v1. White bars represent tissue incubated with PBS as a control, while dashed bars represent tissue incubated in LPS. Error bars represent the coefficient of variation. \* indicates a p-value  $< 0.05$  by Tukey's HSD test, following a two-way ANOVA.

The more ubiquitous form of Basigin, B-v2, was also quantified to determine whether the expression pattern was similar to that of B-v1, as it has been proposed the two isoforms associate to stabilize a lactate metabolon. A similar trend in B-v2 expression was observed, compared to B-v1 in all age groups, though some differences exist. In mice at PD 7, LPS treated tissue expressed more B-v2 than PBS treated tissue, on average ( $p = 4.2 \times 10^{-4}$ ; Figure 3.2A). The time in which the tissue incubated post-treatment had a significant effect of the expression of B-v2 ( $p = 1.2 \times 10^{-6}$ ). That is, tissue incubated for 6 hours expressed significantly more B-v2 than other time points, while tissue incubated for 24 hours expressed significantly less than other time points, regardless of treatment. A significant interaction effect was also observed ( $p = 5.4 \times 10^{-11}$ ). The expression of B-v2 in LPS treated tissue was inversely related to that of B-v2 expression in PBS tissue throughout all incubation periods. An increase in B-v2 was observed for LPS treated tissue at 3- and 12-hour incubation periods, compared to PBS. However, the inverse was observed at the 6- and 24-hour time points.

LPS induced expression of B-v2 in mice at PD 30 was higher than PBS treated tissue ( $p = 2.1 \times 10^{-6}$ ; Figure 3.2 B). Similarly, to B-v1 expression in mice at PD 30, B-v2 transcripts were the most abundant after the 3-hour incubation period ( $p = 9.5 \times 10^{-10}$ ), though no other incubation period indicated a significant response. Additionally, a significant interaction effect was observed ( $p = 7.3 \times 10^{-6}$ ). The expression of B-v2 transcripts were significantly higher in retinal tissue incubated with LPS after 3 and 12 hours, when compared to tissues incubated in PBS for those time points.

In mice at PD 180, B-v2 transcript levels were, on average, more abundant in PBS treated retinal tissue ( $p = 2.1 \times 10^{-6}$ ; Figure 3.2 C). Incubation period showed significant effects ( $p = 8.1 \times 10^{-8}$ ) on B-v2 expression in that at the 3-hour time point transcript levels were the highest, with a significant decline after 6 hours and a significant increase at the 24-hour time point, regardless of treatment. As with most of the treated tissue, a significant interaction was observed in this age group ( $p = 1.6 \times 10^{-9}$ ). B-v2 expression was significantly lower in LPS treated tissue compared to PBS treatment after all incubation periods, except at 12 hours.



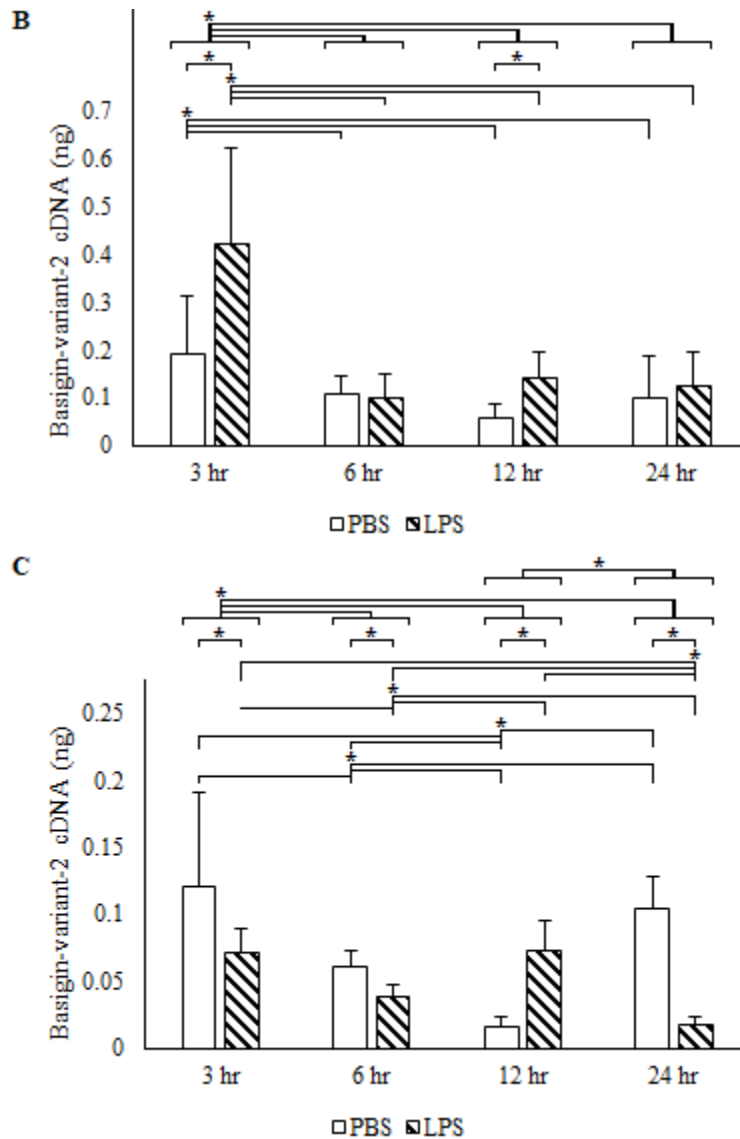


**Figure 3.2 Quantitative analyses of Basigin-variant-2 transcripts in neonate, adolescent, and adult mice.** Quantitative PCR was performed on cDNA isolated from retinal tissue incubated in DMEM  $\pm$  LPS for 3, 6, 12, or 24 hours of mice at PD 7 (A), PD 30 (B) and PD 180 (C), using primers complementary to B-v2. White bars represent tissue incubated with PBS as a control, while dashed bars represent tissue incubated in LPS. Error bars represent the coefficient of variation. \* indicates a p-value  $< 0.05$  by Tukey's HSD test, following a two-way ANOVA.

To identify whether TLR4 transcripts are regulated in the same manner as Basigin gene products in response to an inflammatory stimulus, qPCR was performed to quantify TLR4 cDNA. In mice at PD 7 tissues incubated for 12 hours expressed the highest amount of TLR4, while tissues incubated for 24 hours expressed the least compared to other time points, regardless

of treatment (Figure 3.3A). TLR4 was expressed more, on average, in tissue incubated with LPS than those incubated with PBS ( $p = 1.6 \times 10^{-6}$ ). The time in which the retinal tissue was incubated also had a significant main effect on the expression of TLR4 ( $p = 1.1 \times 10^{-4}$ ). A significant interaction was also observed ( $p = 7.5 \times 10^{-10}$ ). TLR4 transcripts were more abundant in LPS treated tissue after 3 hours of incubation, relative to PBS. However, transcript levels were significantly lower in LPS treated tissue after incubation for 6 and 24 hours, relative to PBS treated tissue. A similar trend was observed in B-v1 and B-v2 expression.

In mice at PD 30, TLR4 expression was higher, on average, in LPS treated retinal tissue compared to PBS treated tissue ( $p = 0.02$ ; Figure 3.3 B). In contrast to B-v1 and B-v2 expression, TLR4 expression was most abundant after the 24-hour incubation period ( $p = 9.2 \times 10^{-10}$ ). A significant interaction was observed ( $p = 0.02$ ), in which TLR4 was significantly lower in tissue incubated for 6 hours, but higher after a 12-hour incubation period, relative to PBS treated tissue.

The trends observed in TLR4 expression of mouse retinal tissue at PD 180 was similar to that observed in B-v1 and B-v2 expression at the same age. TLR4 was more abundant in PBS treated tissue than LPS treated tissue ( $p = 1.1 \times 10^{-11}$ ; Figure 3.3 C), on average. Moreover, the expression of TLR4 transcripts was higher ( $p = 6.1 \times 10^{-12}$ ) at the 3- and 24-hour incubation period when compared to the other two time points. A significant interaction was also determined ( $p = 2.3 \times 10^{-15}$ ). Much like the B-v1 and B-v2 transcripts, TLR4 was more greatly expressed in LPS treated tissue compared to PBS at the 12-hour time point, whereas tissue incubated in PBS expressed more TLR4 than LPS treated tissue at every other incubation period.

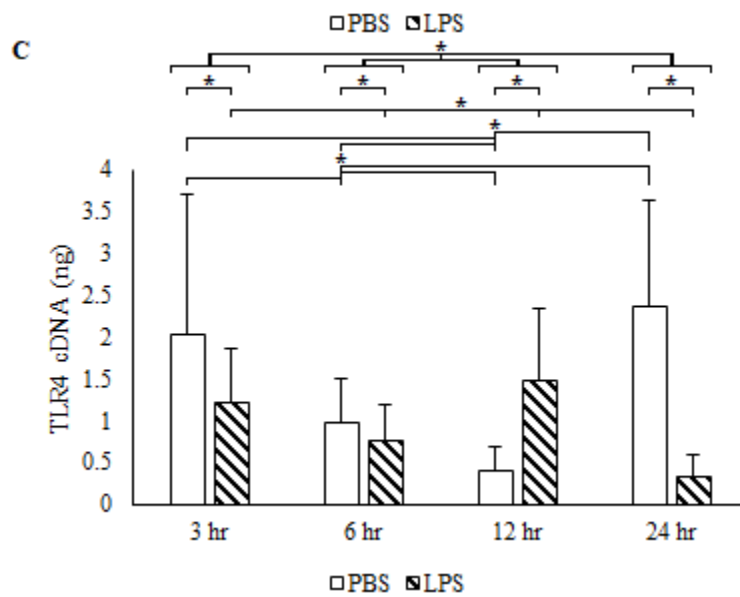
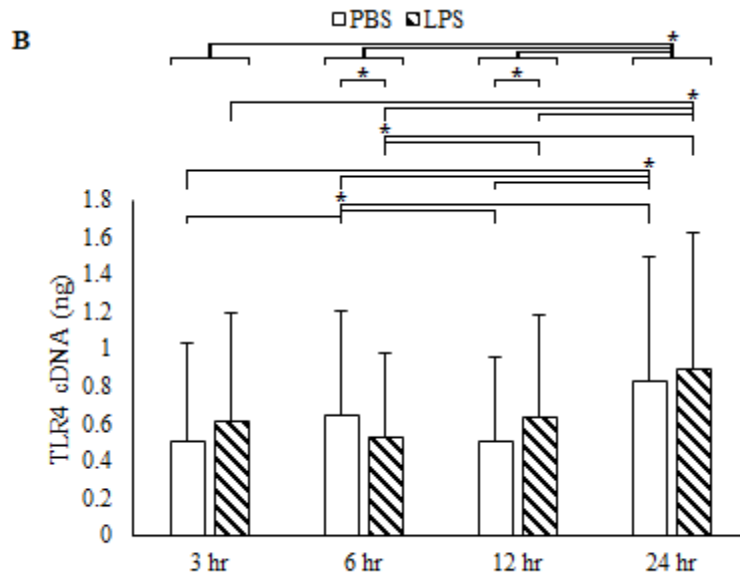
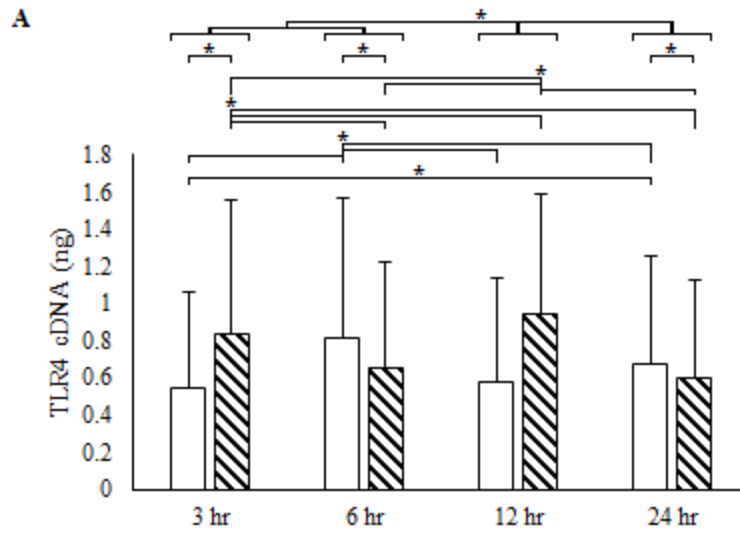


**Figure 3.3 Quantitative analyses of TLR4 transcripts in neonate, adolescent, and adult mice.** Quantitative PCR was performed on cDNA isolated from retinal tissue incubated in DMEM ± LPS for 3, 6, 12, or 24 hours of mice at PD 7 (A), PD 30 (B) and PD 180 (C), using primers complementary to TLR4. White bars represent tissue incubated with PBS as a control, while dashed bars represent tissue incubated in LPS. Error bars represent the coefficient of variation. \* indicates a p-value < 0.05 by Tukey's HSD test, following a two-way ANOVA.

## Discussion

Basigin gene products are essential for the maturation of the eye.<sup>113,114</sup> Basigin-variant-1 (B-v1) is specifically expressed on photoreceptor cells, while Basigin-variant-2 (B-v2) is expressed on the surface of Müller cells, blood vessels, and the retinal pigmented epithelium.<sup>24</sup> Both gene products associate with important metabolic transporters, such as MCTs and GLUT1. Through this association in cis, and the interaction of Basigin gene products in trans, a lactate metabolon is stabilized in the retina.<sup>33</sup> The potential association of B-v2 to TLR4<sup>34</sup> could disrupt the metabolon, depleting the retina of necessary nutrients. Further, the association of B-v2 and TLR4 could stimulate an inflammatory response, exacerbating the degeneration of the retina. Therefore, this study aimed to quantify the expression of Basigin gene products and TLR4 transcripts in the neural retina exposed to an inflammatory stimulus for a varying degree of time in neonatal, adolescent, and adult mice.

The analyses of B-v1 transcripts in neonatal (PD 7) retinal tissue indicated a change in expression when stimulated with LPS. An upregulation in the transcript level was observed during the first 3 hours of incubation, when compared to control (PBS). The considerable decline in B-v1 expression as the incubation period approached 6 hours was determined to be no different to that of PBS treated tissue. However, the over two-fold increase and subsequent decline during the 12- and 24-hour time points, suggest a temporal regulation of B-v1 in response to an inflammatory stressor.

Some similar patterns of transcript expression were observed for B-v2 and TLR4 for this age group in retinal tissue incubated with LPS when compared to control, though differences should be noted. B-v2 transcripts were the most abundant in LPS stimulated tissue at the 3-hour incubation period, rather than 12 hours as seen for B-v1. A rise in B-v2 transcripts were observed at the 6-hour time point in PBS retina, with a decline at 12 hours, which was maintained for the duration of the experiment. Though the shift in expression in tissues incubated with PBS as the incubation period increased suggest an unknown factor is influencing the extent to which B-v2 is expressed, the inverse relationship between PBS and LPS treated tissue is suggestive of the influence LPS may have on the expression of B-v2.

In the adolescent (PD 30) retina, B-v1 transcription differed from that of neonates. The transcript analyses indicated transcription occurred most abundantly during the first 3 hours of incubation in both treatment groups. A continuous decline in the rate of transcription occurred at the 6-hour time point and did not recover until 24 hours. Transcript yield in LPS treated tissue did not differ from those treated with PBS during any incubation period, suggesting LPS does not stimulate the production of B-v1 transcripts at this age. Similarly, B-v2 transcripts were most abundant in the 3-hour incubation period of both treatment groups, but a greater transcript abundance was quantified in retinal tissue incubated with LPS. Additionally, the increase in B-v2 transcripts after 12 hours of LPS incubation suggests a temporal influence of LPS on B-v2 at this age.

The analysis of TLR4 transcripts indicated a similar pattern of expression to that of TLR4 in the neonatal retina, though an increase in both treatment groups was observed at the 24-hour time point. The difference in transcript expression of TLR4 compared to Basigin gene products,

at this age group, suggests a difference in response to an inflammatory stressor. That is, Basigin gene products appear to have a greater response in the short term.

The most varying degree of B-v1 transcript expression was observed in the adult (PD 180) retina. Though the transcript pattern for tissues incubated with PBS mirrored the trend observed in adolescent mice, B-v1 transcription in LPS treated retina was nearly the inverse. During the first 3 hours of incubation, transcripts were considerably lower than that of control tissue. As incubation time increased, B-v1 expression fluctuated with the most abundant transcript level observed at the 12-hour time point, and the lowest at 24 hours. Interestingly, this is the only age group in which B-v2 and B-v1 expression was a direct reflection to that of TLR4. Though further analysis is needed, these initial data indicate a correlation in Basigin gene products and TLR4 expression under the influence of LPS.

## Chapter 4 – Conclusion

Basigin gene products have a dynamic pattern of expression upon stimulation with LPS, dependent on age and length of exposure. In the mouse brain, Basigin was localized to blood vessels in all age groups. However, variation in expression, relative to control tissue, was observed in neonatal and adult, but not adolescent mice, suggesting the adolescent brain may be less susceptible to pathogen invasion. Additionally, the changes that were observed in neonatal and adult mice did not occur during the same period of incubation with LPS, suggesting that the regulation of Basigin due to the length of pathogen exposure is also dependent on age. Due to the unparalleled expression pattern of Basigin and TLR4, Basigin's role in inflammation may be not be associated with TLR4, but other proteins known to initiate an inflammatory response, like CD44.

In the retina, the regulation of Basigin-variant-1 was influenced by the exposure to LPS in neonatal and adult, but not adolescent mice. These data indicate photoreceptor cells of the adolescent retina may be more resilient than these cells at other stages of life. The more ubiquitous form of Basigin, Basigin-variant-2 (B-v2) displayed variation in both a temporal, and age dependent manner. There are various cell types that express B-v2 in the retina, including Müller cells, blood vessels, and the retinal pigmented epithelium.<sup>24</sup> The change in regulation of B-v2 could be a combined effect of these cell types. Basigin gene expression was a direct reflection of TLR4 expression only in the adult retina. Though more analysis is needed, these initial data suggest a correlation between Basigin gene products and TLR4 in the adult retina, but not in other life stages.

Though the mechanism by which Basigin gene products alter the inflammatory response are not known, the data obtained herein indicate a regulatory change to Basigin expression in

response to an inflammatory stressor. It is possible that Basigin is working as a cell adhesion molecule on blood vessels, in which case the downregulation of Basigin gene products in neonates after long-term exposure to LPS indicates this age group is the most vulnerable to attack on the CNS by way of BBB degradation. Another possibility is that Basigin is acting in its role as an inducer of matrix metalloproteinases. To this end, the upregulation of Basigin observed in long-term exposure to LPS in adult brain tissue could be ameliorative, by way of MMP-9 induction and subsequent angiogenesis. The newly formed blood vessels may serve to further protect the central environment from the periphery.

## References

1. Riera Romo M, Pérez-Martínez D, Castillo Ferrer C. 2016. Innate immunity in vertebrates: an overview. *Immunology*. 148(2):125-39.
2. Iwasaki A, Medzhitov R. 2015. Control of adaptive immunity by the innate immune system. *Nat Immunol*. 16(4):343-53.
3. Mahla RS, Reddy MC, Prasad DV, Kumar H. 2013. Sweeten PAMPs: Role of Sugar Complexed PAMPs in Innate Immunity and Vaccine Biology. *Front Immunol*. 4:248.
4. Akira S, Uematsu S, Takeuchi O. 2006. Pathogen recognition and innate immunity. *Cell*. 124(4):783-801.
5. Parham P. 2009. *The Immune System*. Third edition. Garland Science, London. New York: Garland Science, Taylor and Francis Group.
6. Hoshino K, Takeuchi O, Kawai T, Sanjo H, Ogawa T, Takeda Y, Takeda K, Akira S. 1999. Cutting edge: Toll-like receptor 4 (TLR4)-deficient mice are hyporesponsive to lipopolysaccharide: evidence for TLR4 as the Lps gene product. *J Immunol*. 162(7):3749-52.
7. Bella J, Hindle KL, McEwan PA, Lovell SC. 2008. The leucine-rich repeat structure. *Mol Life Sci*. 65:2307-33.
8. Kim HM, Park BS, Kim JI, Kim SE, Lee J, Oh SC, Enkhbayar P, Matsushima N, Lee H, Yoo OJ, Lee JO. 2007. Crystal structure of the TLR4-MD-2 complex with bound endotoxin antagonist Eritoran. *Cell*. 130:906-17.
9. Medzhitov R, Janeway C Jr. 2000. Innate immune recognition: mechanisms and pathways. *Immunol Rev*. 173:89-97.

10. Raetz CR, Whitfield C. 2002. Lipopolysaccharide endotoxins. *Annu Rev Biochem.* 71:635-700.
11. Pugin J, Schürer-Maly CC, Leturcq D, Moriarty A, Ulevitch RJ, Tobias PS. 1993. Lipopolysaccharide activation of human endothelial and epithelial cells is mediated by lipopolysaccharide-binding protein and soluble CD14. *Proc Natl Acad Sci U S A.* 90:2744-8.
12. Chow JC, Young DW, Golenbock DT, Christ WJ, Gusovsky F. 1999. Toll-like receptor-4 mediates lipopolysaccharide-induced signal transduction. *J Biol Chem.* 274:10689-92.
13. Yamamoto M, Sato S, Hemmi H, Sanjo H, Uematsu S, Kaisho T, Hoshino K, Takeuchi O, Kobayashi M, Fujita T, Takeda K, Akira S. 2002. Essential role for TIRAP in activation of the signalling cascade shared by TLR2 and TLR4. *Nature.* 420:324-9.
14. Horng T, Barton GM, Flavell RA, Medzhitov R. 2002. The adaptor molecule TIRAP provides signalling specificity for Toll-like receptors. *Nature.* 420:329-33.
15. Yamamoto M, Sato S, Hemmi H, Hoshino K, Kaisho T, Sanjo H, Takeuchi O, Sugiyama M, Okabe M, Takeda K, Akira S. 2003. Role of adaptor TRIF in the MyD88-independent toll-like receptor signaling pathway. *Science.* 301:640-3.
16. Yamamoto M, Sato S, Hemmi H, Uematsu S, Hoshino K, Kaisho T, Takeuchi O, Takeda K, Akira S. 2003. TRAM is specifically involved in the Toll-like receptor 4-mediated MyD88-independent signaling pathway. *Nat Immunol.* 4:1144-50.
17. Akira S, Takeda K. 2004. Toll-like receptor signalling. *Nat Rev Immunol.* 4:499-511.
18. West AP, Koblansky AA, Ghosh S. 2006. Recognition and signaling by toll-like receptors. *Annu Rev Cell Dev Biol.* 22:409-37.

19. Adhikari A, Xu M, Chen ZJ. 2007. Ubiquitin-mediated activation of TAK1 and IKK. *Oncogene*. 26:3214-26.
20. Chen F, Bhatia D, Chang Q, Castranova V. 2006. Finding NEMO by K63-linked polyubiquitin chain. *Cell Death Differ*. 13:1835-8.
21. Harvey Lodish, Arnold Berk, S Lawrence Zipursky, Paul Matsudaira, David Baltimore, and James Darnell. 2000. *Molecular Cell Biology*. Fourth edition. New York: W. H. Freeman.
22. Bork P, Holm L, Sander C. 1994. The immunoglobulin fold. Structural classification, sequence patterns and common core. *J Mol Biol*. 242(4):309-20.
23. Smith DK, Xue H. 1997. Sequence profiles of immunoglobulin and immunoglobulin-like domains. *J Mol Biol*. 274(4):530-45.
24. Ochrietor JD, Moroz TP, van Ekeris L, Clamp MF, Jefferson SC, deCarvalho AC, Fadool JM, Wistow G, Muramatsu T, Linser PJ. 2003. Retina-specific expression of 5A11/Basigin-2, a member of the immunoglobulin gene superfamily. *Invest Ophthalmol Vis Sci*. 44(9):4086-96.
25. Miyauchi T, Jimma F, Igakura T, Yu S, Ozawa M, Muramatsu T. 1995. Structure of the mouse basigin gene, a unique member of the immunoglobulin superfamily. *J Biochem*. 118(4):717-24.
26. Muramatsu T. 2016. Basigin (CD147), a multifunctional transmembrane glycoprotein with various binding partners. *J Biochem*. 159(5):481-90.
27. Halestrap AP. 2012. The monocarboxylate transporter family--Structure and functional characterization. *IUBMB Life*. 64(1):1-9.

28. Kirk P, Wilson MC, Heddle C, Brown MH, Barclay AN, Halestrap AP. 2000. CD147 is tightly associated with lactate transporters MCT1 and MCT4 and facilitates their cell surface expression. *EMBO J.* 19(15):3896-904.
29. Hori K, Katayama N, Kachi S, Kondo M, Kadomatsu K, Usukura J, Muramatsu T, Mori S, Miyake Y. 2000. Retinal dysfunction in basigin deficiency. *Invest Ophthalmol Vis Sci.* 41(10):3128-33.
30. Poitry-Yamate CL, Poitry S, Tsacopoulos M. 1995. Lactate released by Müller glial cells is metabolized by photoreceptors from mammalian retina. *J Neurosci.* 15(7 Pt 2):5179-91.
31. Philp NJ, Yoon H, Lombardi L. 2001. Mouse MCT3 gene is expressed preferentially in retinal pigment and choroid plexus epithelia. *Am J Physiol Cell Physiol.* 280(5):C1319-26.
32. Gerhart DZ, Leino RL, Drewes LR. 1999. Distribution of monocarboxylate transporters MCT1 and MCT2 in rat retina. *Neuroscience.* 92(1):367-75.
33. Philp NJ, Ochrietor JD, Rudoy C, Muramatsu T, Linser PJ. 2003. Loss of MCT1, MCT3, and MCT4 expression in the retinal pigment epithelium and neural retina of the 5A11/basigin-null mouse. *Invest Ophthalmol Vis Sci.* 44(3):1305-11.
34. Brown JM, Ochrietor JD. 2016. Characterization of the interaction between Basigin and the pattern recognition receptor TLR4. *UNF Digital Commons.* 650.
35. Miyauchi T, Masuzawa Y, Muramatsu T. 1991. The basigin group of the immunoglobulin superfamily: complete conservation of a segment in and around transmembrane domains of human and mouse basigin and chicken HT7 antigen. *J Biochem.* 110(5):770-4.
36. Reese TS, Karnovsky MJ. 1967. Fine structural localization of a blood-brain barrier to exogenous peroxidase. *J Cell Biol.* 34(1):207-17.

37. Abbott NJ, Rönnbäck L, Hansson E. 2006. Astrocyte-endothelial interactions at the blood-brain barrier. *Nat Rev Neurosci.* 7(1):41-53.
38. Virchow R. 1851. Ueber die Erweiterung kleinerer Gefäße. *Archiv f. pathol. Anat.* 3:427–462
39. Robin C. 1859. Recherches sur quelques particularités de la structure des capillaires de l'encephale. *J Physiol Homme Anim.* 2:537–548.
40. Bazzoni G. 2006. Endothelial tight junctions: permeable barriers of the vessel wall. *Thromb Haemost.* 95(1):36-42.
41. Stamatovic SM, Keep RF, Andjelkovic AV. 2008. Brain endothelial cell-cell junctions: how to "open" the blood brain barrier. *Current Neuropharmacology.* 6(3):179–192.
42. Greenwood J, Amos CL, Walters CE, Couraud PO, Lyck R, Engelhardt B, Adamson P. 2003. Intracellular domain of brain endothelial intercellular adhesion molecule-1 is essential for T lymphocyte-mediated signaling and migration. *J Immunol.* 171(4):2099-108.
43. Muller WA, Weigl SA, Deng X, Phillips DM. 1993. PECAM-1 is required for transendothelial migration of leukocytes. *J Exp Med.* 178(2):449-60.
44. Baron JL, Madri JA, Ruddle NH, Hashim G, Janeway CA Jr. 1993. Surface expression of alpha 4 integrin by CD4 T cells is required for their entry into brain parenchyma. *J Exp Med.* 177(1):57-68.
45. Keszthelyi E, Karlik S, Hyduk S, Rice GP, Gordon G, Yednock T, Horner H. 1996. Evidence for a prolonged role of alpha 4 integrin throughout active experimental allergic encephalomyelitis. *Neurology.* 47(4):1053-9.

46. Eugster HP, Frei K, Kopf M, Lassmann H, Fontana A. 1998. IL-6-deficient mice resist myelin oligodendrocyte glycoprotein-induced autoimmune encephalomyelitis. *Eur J Immunol.* 28(7):2178-87.
47. Bettelli E, Carrier Y, Gao W, Korn T, Strom TB, Oukka M, Weiner HL, Kuchroo VK. 2006. Reciprocal developmental pathways for the generation of pathogenic effector TH17 and regulatory T cells. *Nature.* 441(7090):235-8.
48. Bettelli E, Oukka M, Kuchroo VK. 2007. T(H)-17 cells in the circle of immunity and autoimmunity. *Nat Immunol.* 8(4):345-50.
49. Lambrecht BN, Vanderkerken M, Hammad H. 2018. The emerging role of ADAM metalloproteinases in immunity. *Nat Rev Immunol.* 18(12):745-758.
50. Briso EM, Dienz O, Rincon M. 2008. Cutting edge: soluble IL-6R is produced by IL-6R ectodomain shedding in activated CD4 T cells. *J Immunol.* 180(11):7102-6.
51. Pawate S, Shen Q, Fan F, Bhat NR. 2004. Redox regulation of glial inflammatory response to lipopolysaccharide and interferongamma. *J Neurosci Res.* 77(4):540-51.
52. Aslan M, Ozben T. Reactive oxygen and nitrogen species in Alzheimer's disease. 2004. *Curr Alzheimer Res.* 1(2):111-9.
53. Tieu K, Ischiropoulos H, Przedborski S. Nitric oxide and reactive oxygen species in Parkinson's disease. 2003. *IUBMB Life.* 55(6):329-35.
54. Gilgun-Sherki Y, Melamed E, Offen D. The role of oxidative stress in the pathogenesis of multiple sclerosis: the need for effective antioxidant therapy. 2004. *J Neurol.* 251(3):261-8.
55. Gilgun-Sherki Y, Melamed E, Offen D. Oxidative stress induced-neurodegenerative diseases: the need for antioxidants that penetrate the blood brain barrier. 2001. *Neuropharmacology.* 40(8):959-75.

56. Devaskar S, Zahm DS, Holtzclaw L, Chundu K, Wadzinski BE. 1991. Developmental regulation of the distribution of rat brain insulin-insensitive (Glut 1) glucose transporter. *Endocrinology*. 129(3):1530-40.
57. Smith QR, Takasato Y. 1986. Kinetics of amino acid transport at the blood-brain barrier studied using an in situ brain perfusion technique. *Ann N Y Acad Sci*. 481:186-201.
58. Al-Majdoub ZM, Al Feteisi H, Achour B, Warwood S, Neuhoff S, Rostami-Hodjegan A1, Barber J. 2019. Proteomic Quantification of Human Blood-Brain Barrier SLC and ABC Transporters in Healthy Individuals and Dementia Patients. *Mol Pharm*. 16(3):1220-1233.
59. Kuzmich NN, Sivak KV, Chubarev VN, Porozov YB, Savateeva-Lyubimova TN, Peri F. 2017. TLR4 Signaling Pathway Modulators as Potential Therapeutics in Inflammation and Sepsis. *Vaccines (Basel)*. 5(4): E34.
60. Rothaug M, Becker-Pauly C, Rose-John S. 2016. The role of interleukin-6 signaling in nervous tissue. *Biochim Biophys Acta*. 1863(6 Pt A):1218-27.
61. Centers for Disease Control and Prevention. 2018. Life expectancy at birth, at age 65, and at age 75, by sex, race, and Hispanic origin: United States, selected years 1900–2017. <https://www.cdc.gov/nchs/data/hus/2018/004.pdf>
62. Hirsch L, Jette N, Frolkis A, Steeves T, Pringsheim T. 2016. The Incidence of Parkinson's Disease: A Systematic Review and Meta-Analysis. *Neuroepidemiology*. 46(4):292-300.
63. Alzheimer's Association. 2016. 2016 Alzheimer's disease facts and figures. *Alzheimers Dement*. 12(4):459-509.
64. Wallin MT, Culpepper WJ, Campbell JD, Nelson LM, Langer-Gould A, Marrie RA, Cutter GR, Kaye WE, Wagner L, Tremlett H, Buka SL, Dilokthornsakul P, Topol B, Chen LH,

- LaRocca NG. 2019. The prevalence of MS in the United States: A population-based estimate using health claims data. *Neurology*. 92(10):e1029-e1040.
65. Kettenmann H, Hanisch UK, Noda M, Verkhratsky A. 2011. Physiology of microglia. *Physiol Rev*. 91(2):461-553.
66. Popovich PG, Longbrake EE. 2008. Can the immune system be harnessed to repair the CNS? *Nat Rev Neurosci*. 9(6):481-93.
67. Lull ME, Block ML. 2010. Microglial activation and chronic neurodegeneration. *Neurotherapeutics*. 7(4):354-65.
68. Qin L, Liu Y, Wang T, Wei SJ, Block ML, Wilson B, Liu B, Hong JS. 2004. NADPH oxidase mediates lipopolysaccharide-induced neurotoxicity and proinflammatory gene expression in activated microglia. *J Biol Chem*. 279(2):1415-21.
69. Circu ML, Aw TY. 2010. Reactive oxygen species, cellular redox systems, and apoptosis. *Free Radic Biol Med*. 48(6):749-62.
70. Babior BM. 2000. Phagocytes and oxidative stress. *Am J Med*. 109(1):33-44.
71. Doussi re J, Gaillard J, Vignais PV. 1996. Electron transfer across the O<sub>2</sub>- generating flavocytochrome b of neutrophils. Evidence for a transition from a low-spin state to a high-spin state of the heme iron component. *Biochemistry*. 35(41):13400-10.
72. Mattson MP. 1998. Modification of ion homeostasis by lipid peroxidation: roles in neuronal degeneration and adaptive plasticity. *Trends Neurosci*. 21(2):53-7.
73. Kim YS, Choi DH, Block ML, Lorenzl S, Yang L, Kim YJ, Sugama S, Cho BP, Hwang O, Browne SE, Kim SY, Hong JS, Beal MF, Joh TH. 2007. A pivotal role of matrix metalloproteinase-3 activity in dopaminergic neuronal degeneration via microglial activation. *FASEB J*. 21(1):179-87.

74. Zecca L, Zucca FA, Wilms H, Sulzer D. 2003. Neuromelanin of the substantia nigra: a neuronal black hole with protective and toxic characteristics. *Trends Neurosci.* 26(11):578-80.
75. Zhang W, Wang T, Pei Z, Miller DS, Wu X, Block ML, Wilson B, Zhang W, Zhou Y, Hong JS, Zhang J. 2005. Aggregated alpha-synuclein activates microglia: a process leading to disease progression in Parkinson's disease. *FASEB J.* 19(6):533-42.
76. Lin HW, Levison SW. 2009. Context-dependent IL-6 potentiation of interferon- gamma-induced IL-12 secretion and CD40 expression in murine microglia. *J Neurochem.* 111(3):808-18.
77. Zuchero YJ, Chen X, Bien-Ly N, Bumbaca D, Tong RK, Gao X, Zhang S, Hoyte K, Luk W, Huntley MA, Phu L, Tan C, Kallop D, Weimer RM, Lu Y, Kirkpatrick DS, Ernst JA, Chih B, Dennis MS, Watts RJ. 2016. Discovery of Novel Blood-Brain Barrier Targets to Enhance Brain Uptake of Therapeutic Antibodies. *Neuron.* 89(1):70-82.
78. Sameshima T, Nabeshima K, Toole BP, Inoue T, Yokogami K, Nakano S, Ohi T, Wakisaka S. 2003. Correlation of emmprin expression in vascular endothelial cells with blood-brain-barrier function: a study using magnetic resonance imaging enhanced by Gd-DTPA and immunohistochemistry in brain tumors. *Virchows Arch.* 442(6):577-84.
79. Yurchenko V, Constant S, Eisenmesser E, Bukrinsky M. 2010. Cyclophilin-CD147 interactions: a new target for anti-inflammatory therapeutics. *Clin Exp Immunol.* 160(3):305-17.
80. Xu Q, Leiva MC, Fischkoff SA, Handschumacher RE, Lyttle CR. 1992. Leukocyte chemotactic activity of cyclophilin. *J Biol Chem.* 267(17):11968-71.

81. Kato N, Yuzawa Y, Kosugi T, Hobo A, Sato W, Miwa Y, Sakamoto K, Matsuo S, Kadomatsu K. 2009. The E-selectin ligand basigin/CD147 is responsible for neutrophil recruitment in renal ischemia/reperfusion. *J Am Soc Nephrol.* 20(7):1565-76.
82. Grass GD, Tolliver LB, Bratoeva M, Toole BP. 2013. CD147, CD44, and the epidermal growth factor receptor (EGFR) signaling pathway cooperate to regulate breast epithelial cell invasiveness. *J Biol Chem.* 288(36):26089-104.
83. Kim MY, Cho JY. 2016. Molecular association of CD98, CD29, and CD147 critically mediates monocytic U937 cell adhesion. *Korean J Physiol Pharmacol.* 20(5):515-23.
84. Reynolds JM, Martinez GJ, Chung Y, Dong C. 2012. Toll-like receptor 4 signaling in T cells promotes autoimmune inflammation. *Proc Natl Acad Sci U S A.* 109(32):13064-9.
85. Li Q, Cherayil BJ. 2003. Role of Toll-like receptor 4 in macrophage activation and tolerance during *Salmonella enterica* serovar Typhimurium infection. *Infect Immun.* 71(9):4873-82.
86. Lu Z, Li Y, Jin J, Zhang X, Lopes-Virella MF, Huang Y. 2012. Toll-like receptor 4 activation in microvascular endothelial cells triggers a robust inflammatory response and cross talk with mononuclear cells via interleukin-6. *Arterioscler Thromb Vasc Biol.* 32(7):1696-706.
87. Igakura T, Kadomatsu K, Kaname T, Muramatsu H, Fan QW, Miyauchi T, Toyama Y, Kuno N, Yuasa S, Takahashi M, Senda T, Taguchi O, Yamamura K, Arimura K, Muramatsu T. 1998. A null mutation in basigin, an immunoglobulin superfamily member, indicates its important roles in peri-implantation development and spermatogenesis. *Dev Biol.* 194(2):152-65.
88. Mannowetz N, Wandernoth P, Wennemuth G. 2012. Basigin interacts with both MCT1 and MCT2 in murine spermatozoa. *J Cell Physiol.* 227(5):2154-62.

89. Kumagai AK. Glucose transport in brain and retina: implications in the management and complications of diabetes. 1999. *Diabetes Metab Res Rev.* 15(4):261-73.
90. Besse F, Mertel S, Kittel RJ, Wichmann C, Rasse TM, Sigrist SJ, Ephrussi A. 2007. The Ig cell adhesion molecule Basigin controls compartmentalization and vesicle release at *Drosophila melanogaster* synapses. *J Cell Biol.* 177(5):843-55.
91. Till A, Rosenstiel P, Bräutigam K, Sina C, Jacobs G, Oberg HH, Seegert D, Chakraborty T, Schreiber S. 2008. A role for membrane-bound CD147 in NOD2-mediated recognition of bacterial cytoinvasion. *J Cell Sci.* 121(Pt 4):487-95.
92. Dawar FU, Xiong Y, Khattak MNK, Li J, Lin L, Mei J. 2017. Potential role of cyclophilin A in regulating cytokine secretion. *J Leukoc Biol.* 102(4):989-992.
93. Roulet MJ, Mongo KG, Vassort G, Ventura-Clapier R. 1979. The dependence of twitch relaxation on sodium ions and on internal Ca<sup>2+</sup> stores in voltage clamped frog atrial fibres. *Pflugers Arch.* 379(3):259-68.
94. Ke X, Chen Y, Wang P, Xing J, Chen Z. 2014. Upregulation of CD147 protects hepatocellular carcinoma cell from apoptosis through glycolytic switch via HIF-1 and MCT-4 under hypoxia. *Hepatol Int.* 8(3):405-14.
95. Gedeon T, Bokes P. 2012. Delayed protein synthesis reduces the correlation between mRNA and protein fluctuations. *Biophys J.* 103(3):377-385.
96. Bratsun D, Volfson D, Tsimring LS, Hasty J. 2005. Delay-induced stochastic oscillations in gene regulation. *Proc Natl Acad Sci U S A.* 102(41):14593-8.
97. Jayakumar AR, Tong XY, Curtis KM, Ruiz-Cordero R, Abreu MT, Norenberg MD. 2014. Increased toll-like receptor 4 in cerebral endothelial cells contributes to the astrocyte swelling and brain edema in acute hepatic encephalopathy. *J Neurochem.* 128(6):890-903.

98. Savani RC, Cao G, Pooler PM, Zaman A, Zhou Z, DeLisser HM. 2001. Differential involvement of the hyaluronan (HA) receptors CD44 and receptor for HA-mediated motility in endothelial cell function and angiogenesis. *J Biol Chem.* 276(39):36770-8.
99. Bourne RR, Stevens GA, White RA, Smith JL, Flaxman SR, Price H, Jonas JB, Keeffe J, Leasher J, Naidoo K, Pesudovs K, Resnikoff S, Taylor HR. 2013. Causes of vision loss worldwide, 1990-2010: a systematic analysis. *Lancet Glob Health.* 1(6):e339-49.
100. Wilkinson CP, Ferris FL 3rd, Klein RE, Lee PP, Agardh CD, Davis M, Dills D, Kampik A, Pararajasegaram R, Verdaguer JT. 2003. Proposed international clinical diabetic retinopathy and diabetic macular edema disease severity scales. *Ophthalmology.* 110(9):1677-82.
101. Stitt AW, Lois N, Medina RJ, Adamson P, Curtis TM. 2013. Advances in our understanding of diabetic retinopathy. *Clin Sci (Lond).* 125(1):1-17.
102. Ford JA, Lois N, Royle P, Clar C, Shyangdan D, Waugh N. 2013. Current treatments in diabetic macular oedema: systematic review and meta-analysis. *BMJ Open.* 3(3):e002269.
103. Yu Y, Chen H, Su SB. 2015. Neuroinflammatory responses in diabetic retinopathy. *J Neuroinflammation.* 12:141.
104. Fuhrmann S. 2010. Eye morphogenesis and patterning of the optic vesicle. *Curr Top Dev Biol.* 93:61-84.
105. Jacobson M, Hirose G. 1978. Origin of the retina from both sides of the embryonic brain: a contribution to the problem of crossing at the optic chiasma. *Science.* 202(4368):637-9.
106. Ahmed J, Braun RD, Dunn R Jr, Linsenmeier RA. 1993. Oxygen distribution in the macaque retina. *Invest Ophthalmol Vis Sci.* 34(3):516-21.

107. Nickla DL, Wallman J. 2009. The multifunctional choroid. *Prog Retin Eye Res.* 29(2):144-68.
108. Campbell M, Humphries P. 2012. The blood-retina barrier: tight junctions and barrier modulation. *Adv Exp Med Biol.* 763:70-84.
109. Mantych GJ, Hageman GS, Devaskar SU. 1993. Characterization of glucose transporter isoforms in the adult and developing human eye. *Endocrinology.* 133(2):600-7.
110. Kumagai AK, Glasgow BJ, Pardridge WM. 1994. GLUT1 glucose transporter expression in the diabetic and nondiabetic human eye. *Invest Ophthalmol Vis Sci.* 35(6):2887-94.
111. Winkler BS, Arnold MJ, Brassell MA, Puro DG. 2000. Energy metabolism in human retinal Müller cells. *Invest Ophthalmol Vis Sci.* 41(10):3183-90.
112. Finch NA, Linser PJ, Ochrietor JD. 2009. Hydrophobic interactions stabilize the basigin-MCT1 complex. *Protein J.* 28(7-8):362-8.
113. Ochrietor JD, Moroz TM, Kadomatsu K, Muramatsu T, Linser PJ. 2001. Retinal degeneration following failed photoreceptor maturation in 5A11/basigin null mice. *Exp Eye Res.* 72(4):467-77.
114. Ochrietor JD, Moroz TP, Clamp MF, Timmers AM, Muramatsu T, Linser PJ. 2002. Inactivation of the Basigin gene impairs normal retinal development and maturation. *Vision Res.* 42(4):447-53.

## Vita

- Name of author:** Alicia I. Gonzalez
- Date and place of birth:** Redacted 1991 Miami, Florida
- Degrees awarded:** A.A. Criminal Justice, Miami Dade College, 2012  
B.S. Psychology, Florida State University, 2015
- Honors and Awards:** UNF Biology Graduate Summer Research Grant, 2018  
UNF Graduate School Research Grant, 2019  
ASCB Minority Affairs Committee Travel Award, 2019
- Presentations:** Alicia Gonzalez and Judith D Ochrietor  
Basigin: A Novel Cell-Adhesion System and Immune Response Stimulant in the Neural Retina  
University of North Florida SOARS poster session, 2019.  
Jacksonville, FL
- Alicia Gonzalez and Judith D Ochrietor  
Basigin gene products associate to form a novel cell-adhesion system used to maintain a metabolic cytoarchitecture and potentially stimulate an immune response in the neural retina  
Experimental Biology (EB) Conference, 2019.  
Orlando, FL
- Alicia Gonzalez and Judith D Ochrietor  
The Role of Basigin as an immune mediator in the CNS  
American Society for Cell Biology (ASCB) Conference, 2019.  
Washington, D.C.
- Alicia Gonzalez and Judith D Ochrietor  
The Role of Basigin as an immune mediator in the CNS  
University of North Florida SOARS poster session, 2020.  
Jacksonville, FL

CERTIFICATE OF APPROVAL

The thesis “Basigin as an immune mediator in the CNS” submitted by Alicia Gonzalez

Approved by the thesis committee:

Date:

---

Dr. Judith Ochrietor  
Committee Chair Person

---

Dr. Fatima Rehman

---

Dr. Beth Stotz-Potter